

International Journal of Systems Science

ISSN: 0020-7721 (Print) 1464-5319 (Online) Journal homepage: www.tandfonline.com/journals/tsys20

Output emulator-based observer-free distributed output feedback adaptive control for multivehicle systems

Ali Albattat & Tansel Yucelen

To cite this article: Ali Albattat & Tansel Yucelen (13 Jul 2026): Output emulator-based observer-free distributed output feedback adaptive control for multivehicle systems, International Journal of Systems Science, DOI: 10.1080/00207721.2026.2685307

To link to this article: https://doi.org/10.1080/00207721.2026.2685307

Published online: 13 Jul 2026.

Submit your article to this journal

Article views: 66

View related articles

View Crossmark data

Full Terms & Conditions of access and use can be found at
https://www.tandfonline.com/action/journalInformation?journalCode=tsys20

INTERNATIONAL JOURNAL OF SYSTEMS SCIENCE
https://doi.org/10.1080/00207721.2026.2685307

Taylor & Francis
by informa

Check for updates

Output emulator-based observer-free distributed output feedback adaptive control for multivehicle systems

Ali Albattat[a] and Tansel Yucelen[b]

[a]Department of Mechanical Engineering, University of Al-Qadisiyah, Al-Qadisiyah, Iraq; [b]Department of Mechanical Engineering and the Director of the Laboratory for Autonomy, Control, Information, and Systems (LACIS, (http://lacis.eng.usf.edu/), University of South Florida, Tampa, FL, USA

ABSTRACT

In this work, we develop a novel output emulator-based, observer-free output feedback adaptive control ((OF)^{2}AC) method designed for continuous-time, minimum phase, and high-order linear multivehicle systems in the presence of exogenous disturbances, specifically addressing the containment problem. The (OF)^{2}AC framework leverages a nonminimal state-space representation for each follower vehicle, wherein this formulation generates an extended set of states by utilising the filtered inputs, filtered outputs, and their respective derivatives of the follower vehicles, thus eliminating the need for observer design for each individual vehicle. Moreover, the output emulator reference model is employed to ensure smooth transient behaviour by mitigating potential high-frequency oscillations. A Lyapunov-based analysis establishes uniform ultimate boundedness of the overall closed-loop system in the presence of exogenous disturbances. To demonstrate the efficacy of the proposed methodology, two numerical examples involving containment control scenarios are provided.

ARTICLE HISTORY
Received 3 January 2026
Accepted 31 May 2026

KEYWORDS
Adaptive control; output feedback; output emulator; multivehicle systems; containment control

1. Introduction

Multivehicle systems, which consist of interconnected mobile dynamical systems, facilitate collaborative tasks by exchanging status information through network protocols. Their applications span various domains, including civil and military sectors, for tasks such as rescue operations and controlling clusters of satellites and telescopes (Kim et al., 2004; Mesbahi & Egerstedt, 2010; Olfati-Saber et al., 2007; Ren et al., 2005).

Vehicle system models, typically derived from fundamental physical laws, encounter discrepancies with actual systems due to simplifications stemming from complexity, nonlinearity, and uncertainty. Cooperative control designs must address these discrepancies to achieve system-level objectives while ensuring stability amidst uncertainty (Sun & Geng, 2016; Wang et al., 2014; Yucelen & Johnson, 2013). However, achieving full state feedback, essential for proposed controllers, requires knowledge of system state variables, which is impractical for multivehicle systems with unknown state variables. Consequently, output feedback architectures are essential for applications that involve high-dimensional systems with unknown state variables, including systems such as fleets of unmanned aerial vehicles, mobile robotic platforms, and robotic manipulators.

To address this challenge, the works of Hu and Zheng (2014), Peng et al. (2014), Cai et al. (2017) and Sun et al. (2016) propose adaptive output feedback controllers for dynamical multivehicle systems with uncertainties. Specifically, in Hu and Zheng (2014), Peng et al. (2014) and Cai et al. (2017), adaptive output feedback controllers are developed for consensus protocols, where the control gains depend on the global network information, represented by the Laplacian matrix. The authors of Sun et al. (2016) introduce two observer designs a local observer and an adaptive estimator for distributed adaptive output-feedback consensus tracking in systems with unknown agent dynamics, without relying on Laplacian matrix information. A common characteristic among these works is that adaptive output feedback controllers utilise observers to estimate unknown state variables.

While the use of nonminimal state-space realisation for observer-free output feedback control has

CONTACT Ali Albattat ali.albattat@qu.edu.iq Department of Mechanical Engineering, University of Al-Qadisiyah, Al-Qadisiyah 58002, Iraq

© 2026 Informa UK Limited, trading as Taylor & Francis Group

been introduced in Yucelen and Haddad (2012), its significance relative to conventional observer-based approaches warrants further clarification. Classical output feedback adaptive control methods typically rely on high-gain observers or output predictors to estimate unmeasured states, which introduces additional dynamics and increases sensitivity to measurement noise. Moreover, such approaches often require restrictive assumptions, including minimum-phase behaviour and knowledge of system relative degree.

In contrast, the observer-free framework adopted in this work eliminates the need for explicit state estimation by employing a nonminimal state-space realisation. This significantly reduces implementation complexity, avoids observer gain tuning, and mitigates the amplification of high-frequency measurement noise. These advantages are particularly important in multivehicle systems, where distributed implementation and reduced sensitivity to measurement noise are critical.

In a recent study (Albattat, Yucelen, et al., 2017), we developed an output feedback control framework for dynamical multivehicle systems that operates without the use of observers, extending beyond the scope of adaptive control. This observer-free architecture builds upon the initial concept of observer-free output feedback adaptive control introduced in Yucelen and Haddad (2012). In a subsequent advancement (Albattat et al., 2018), we introduced an observer-free output feedback adaptive control method, referred to as $(OF)^2AC$, specifically designed for continuous-time, minimum phase, and high-order linear multivehicle systems subject to exogenous disturbances. Similar to the observer-free methods presented in Yucelen and Haddad (2012) and Albattat, Yucelen, et al. (2017), the $(OF)^2AC$ utilises a nonminimal state-space realisation for each follower vehicle. This realisation produces an expanded state set by incorporating filtered inputs, filtered outputs, and their derivatives. The $(OF)^2AC$ framework includes (i) a local cooperative controller, as discussed in Yucelen and Johnson (2013), and (ii) a vehicle-level controller for each follower vehicle. Specifically, part (i) addresses the leader-follower containment control problem by utilising relative output measurements from neighbouring vehicles, while part (ii) consists of an adaptive controller that provides stabilisation and command following in the presence of exogenous disturbances.

However, despite the advantages of observer-free output feedback adaptive control, the use of high-gain adaptation mechanisms may introduce undesirable high-frequency oscillations in the control signal, particularly in the presence of uncertainties and disturbances. To address this limitation, the key contribution of this paper is the introduction of a novel output emulator-based approach that leverages an output emulator reference model to mitigate high-frequency oscillations in the control signal. The proposed method is inspired by state emulator adaptive control (Albattat, Gruenwald, et al., 2017; Gibson et al., 2012a, 2012b; Lavretsky et al., 2010) and provides an alternative to low-pass filter-based learning approaches. Compared to the previously proposed low-frequency learning method (Yucelen & Haddad, 2013), the proposed output emulator-based approach requires fewer tuning parameters, simplifies implementation, and improves control signal smoothness without introducing additional tuning complexity. A preliminary version of this work was presented in our earlier conference paper (Albttat & Yucelen, 2025), where we first introduced the output emulator-based observer-free distributed output feedback adaptive control $(OF)^2AC$ framework and demonstrated its feasibility using a simplified numerical example. The present journal article significantly extends that study by providing a complete theoretical formulation, detailed stability analysis, and comprehensive simulation results to validate the proposed approach.

The main contributions of this paper can be summarised as follows. First, an observer-free distributed output feedback adaptive control framework is developed for multivehicle systems using nonminimal state-space realisation, eliminating the need for explicit state observers. Second, a novel output emulator-based approach is developed to mitigate high-frequency oscillations in the control signal arising from high-gain adaptive mechanisms. Third, a rigorous stability analysis is established for the overall closed-loop multivehicle system. Finally, the effectiveness of the proposed approach is demonstrated through numerical examples, including containment control scenarios with both single-leader and two-leader cases.

The structure of the paper is as follows. Section 2 introduces the notation used throughout the paper and reviews some fundamental concepts from multivehicle

systems. In Section 3, a nonminimal state-space realisation technique, as presented in Yucelen and Haddad (2012), is discussed. The proposed control method is outlined in Section 4. Section 5 provides the stability analysis for the overall multivehicle system. Two numerical examples are presented in Section 6 to demonstrate the effectiveness of the proposed control framework. Finally, Section 7 offers concluding remarks.

2. Notation and mathematical preliminaries

The notation used in this paper is fairly standard and similar to, for example, our earlier work in Albattat, Yucelen, et al. (2017). For self-containedness, $\mathbb{R}$ denotes the set of real numbers, $\mathbb{R}^n$ denotes the set of $n \times 1$ real column vectors, $\mathbb{R}^{n\times m}$ denotes the set of $n \times m$ real matrices, $\mathbb{R}_+$ denotes the set of positive real numbers, $\mathbb{R}_+^{n\times n}$ denotes the set of $n \times n$ positive-definite real matrices, $\mathbb{S}^{n\times n}$ denotes the set of $n \times n$ symmetric real matrices, $\mathbb{D}^{n\times n}$ denotes the set of $n \times n$ real matrices with diagonal scalar entries, $(\cdot)^{\mathrm{T}}$ denotes transpose, $(\cdot)^{-1}$ denotes inverse, $(\cdot)^{\dagger}$ denotes Pseudo inverse, $\mathrm{diag}(a)$ denotes the diagonal matrix with the vector a on its diagonal, and '$\triangleq$' denotes equality by definition. In addition, we write $\lambda_{\min}(A)$ (respectively, $\lambda_{\max}(A)$) for the minimum and respectively maximum eigenvalue of the Hermitian matrix A, $\|\cdot\|$ for the Euclidean norm, and $\|\cdot\|_{\mathrm{F}}$ for the Frobenius matrix norm.

Additionally, we employ graph-theoretical notation, as outlined in foundational texts (e.g. Godsil & Royle, 2001; Mesbahi & Egerstedt, 2010), to represent the interactions among vehicles. Specifically, an undirected graph $\mathcal{G}$ is defined by a set of nodes $\mathcal{V}_{\mathcal{G}} = \{1, \ldots, N\}$ and a set of edges $\mathcal{E}_{\mathcal{G}} \subseteq \mathcal{V}_{\mathcal{G}} \times \mathcal{V}_{\mathcal{G}}$. If $(i, j) \in \mathcal{E}_{\mathcal{G}}$, then nodes i and j are considered neighbours, denoted by $i \sim j$. The degree d_i of node i corresponds to the number of its neighbours, and the degree matrix of graph $\mathcal{G}$ is given by $\mathcal{D}(\mathcal{G}) \triangleq \mathrm{diag}(d) \in \mathbb{R}^{N\times N}$, where $d = [d_1, \ldots, d_N]^{\mathrm{T}}$. A path $i_0 i_1 \cdots i_L$ is a finite sequence of nodes such that $i_{k-1} \sim i_k$ for $k = 1, \ldots, L$, and if there exists a path between any pair of distinct nodes, the graph $\mathcal{G}$ is considered connected. Additionally, the adjacency matrix of a graph $\mathcal{G}$ is denoted as $\mathcal{A}(\mathcal{G}) \in \mathbb{R}^{N\times N}$, defined by

$$[\mathcal{A}(\mathcal{G})]_{ij} \triangleq \begin{cases} 1, & \text{if } (i, j) \in \mathcal{E}_{\mathcal{G}} \\ 0, & \text{otherwise,} \end{cases} \tag{1}$$

and $\mathcal{B}(\mathcal{G}) \in \mathbb{R}^{N\times M}$ for the (node-edge) incidence matrix of the graph $\mathcal{G}$ defined by

$$[\mathcal{B}(\mathcal{G})]_{ij} \triangleq \begin{cases} 1, & \text{if node } i \text{ is the head of the edge } j, \\ -1, & \text{if node } i \text{ is the tail of the edge } j, \\ 0, & \text{otherwise,} \end{cases} \tag{2}$$

where M is the number of edges, i is an index for the node set, and j is an index for the edge set. Finally, the graph Laplacian matrix, $\mathcal{L}(\mathcal{G}) \in \overline{\mathbb{R}}_+^{N\times N} \cap \mathbb{S}^{N\times N}$, is defined by

$$\mathcal{L}(\mathcal{G}) \triangleq \mathcal{D}(\mathcal{G}) - \mathcal{A}(\mathcal{G}), \tag{3}$$

or equivalently,

$$\mathcal{L}(\mathcal{G}) = \mathcal{B}(\mathcal{G})\mathcal{B}(\mathcal{G})^{\mathrm{T}}. \tag{4}$$

Next, we review some fundamental results pertaining to first-order multivehicle systems (Mesbahi & Egerstedt, 2010). In particular, nodes and edges are used to represent the vehicles and the information exchange links between them, respectively. Consequently, a multivehicle system can be modeled as a graph $\mathcal{G}$. For instance, let the state of node i, where $i = 1, \ldots, N$, be represented by $x_i(t) \in \mathbb{R}$, satisfying

$$\dot{x}_i(t) = u_i(t), \quad x_i(0) = x_{i0}, \tag{5}$$

where $u_i(t) \in \mathbb{R}$ represents the control input. The model in (5) is introduced as a simple first-order integrator to illustrate basic coordination concepts in multivehicle systems. It does not represent the class of systems addressed in this paper. The proposed control framework is developed for a more general class of higher-order uncertain systems (see Section 3). Accordingly, the preliminary model is used only to define coordination objectives, while the main results address significantly more complex and realistic system dynamics. If each vehicle has access to the relative state information of its neighbours, then

$$u_i(t) = -\sum_{i\sim j} \big(x_i(t) - x_j(t)\big), \tag{6}$$

solves the rendezvous problem. With (5) subject to (6), the system dynamics for the entire multivehicle system can be expressed as

$$\dot{x}(t) = -\mathcal{L}(\mathcal{G})x(t), \quad x_i(0) = x_{i0}, \tag{7}$$

where $x(t) = [x_1^{\mathrm{T}}(t), \ldots, x_N^{\mathrm{T}}(t)]$ represents the aggregated state vector. The spectrum of $\mathcal{L}(\mathcal{G})$ includes one zero eigenvalue and $N-1$ positive real eigenvalues if, and only if, the graph $\mathcal{G}$ is connected and undirected. Under these conditions, the solution to the multivehicle system described by (7) converges as $x(t) \to (\mathbf{1}_N \mathbf{1}_N^{\mathrm{T}}/N)x_0$ as $t \to \infty$.

Additionally, we recall some key results regarding leader-follower frameworks. Let the incidence matrix in (2) be partitioned as follows:

$$\mathcal{B}(\mathcal{G}) = \begin{bmatrix} \mathcal{B}_{\mathrm{L}}(\mathcal{G}) \\ \mathcal{B}_{\mathrm{F}}(\mathcal{G}) \end{bmatrix}, \tag{8}$$

where $\mathcal{B}_{\mathrm{L}}(\mathcal{G}) \in \mathbb{R}^{N_{\mathrm{L}} \times M}$ and $\mathcal{B}_{\mathrm{F}}(\mathcal{G}) \in \mathbb{R}^{N_{\mathrm{F}} \times M}$, with N_{L} and N_{F} representing the number of leader and follower nodes, respectively, such that $N = N_{\mathrm{L}} + N_{\mathrm{F}}$. Utilising (4) and (8), the partitioned graph Laplacian matrix $\mathcal{L}(\mathcal{G})$ can be expressed as

$$\mathcal{L}(\mathcal{G}) = \begin{bmatrix} L(\mathcal{G}) & G(\mathcal{G})^{\mathrm{T}} \\ G(\mathcal{G}) & F(\mathcal{G}) \end{bmatrix}, \tag{9}$$

where $L(\mathcal{G}) \triangleq \mathcal{B}_{\mathrm{L}}(\mathcal{G})\mathcal{B}_{\mathrm{L}}(\mathcal{G})^{\mathrm{T}}$, $G(\mathcal{G}) = \mathcal{B}_{\mathrm{F}}(\mathcal{G})\mathcal{B}_{\mathrm{L}}(\mathcal{G})^{\mathrm{T}}$, and $F(\mathcal{G}) = \mathcal{B}_{\mathrm{F}}(\mathcal{G})\mathcal{B}_{\mathrm{F}}(\mathcal{G})^{\mathrm{T}}$. Note that $F(\mathcal{G}) \in \mathbb{R}_+^{N_{\mathrm{F}} \times N_{\mathrm{F}}} \cap \mathbb{S}^{N_{\mathrm{F}} \times N_{\mathrm{F}}}$, and since $\det(F(\mathcal{G})) \neq 0$, $F(\mathcal{G})$ is nonsingular. Furthermore, $F(\mathcal{G})\mathbf{1}_{N\mathrm{F}} = -G(\mathcal{G})\mathbf{1}_{N\mathrm{L}}$, meaning that each row of $-F(\mathcal{G})^{\mathrm{T}}G(\mathcal{G})$ has a sum of 1. Now, we can represent the multivehicle system using a leader-follower framework. Specifically, let $x_{\mathrm{L}}(t) \in \mathbb{R}^{N_{\mathrm{L}}}$ and $x_{\mathrm{F}}(t) \in \mathbb{R}^{N_{\mathrm{F}}}$ denote the aggregated state vectors of the leaders and followers, respectively. The dynamics of the followers evolve according to the Laplacian-based model as

$$\dot{x}_{\mathrm{F}}(t) = -F(\mathcal{G})x_{\mathrm{F}}(t) - G(\mathcal{G})x_{\mathrm{L}}(t), \quad x_{\mathrm{F}}(0) = x_{\mathrm{F}0}. \tag{10}$$

Throughout this paper, the leaders are treated as command generators for their neighbouring followers, and the interaction topology among vehicles is modeled by a connected, undirected graph $\mathcal{G}$.

Finally, we provide the following definition necessary for the main results in this paper.

Definition 2.1: Let $\phi : \mathbb{R}^n \to \mathbb{R}$ be a continuously differentiable convex function given by $\phi(\theta) \triangleq ((\epsilon_\theta + 1)\theta^T \cdot \theta - \theta_{\max}^2)/(\epsilon_\theta \theta_{\max}^2)$, where $\theta_{\max} \in \mathbb{R}$ is a projection norm bound imposed on $\theta \in \mathbb{R}^n$ and $\epsilon > 0$ is a projection tolerance bound. Then, for $y \in \mathbb{R}^n$, the projection operator $\mathrm{Proj} : \mathbb{R}^n \times \mathbb{R}^n \to \mathbb{R}^n$ is defined by

$$\mathrm{Proj}(\theta, y) \triangleq \begin{cases} y, & \text{if } \phi(\theta) < 0, \\ y, & \text{if } \phi(\theta) \geq 0 \text{ and } \phi'(\theta) y \leq 0, \\ y - \dfrac{\phi'^{\mathrm{T}}(\theta)\phi'(\theta)y}{\phi'(\theta)\phi'^{\mathrm{T}}(\theta)}\phi(\theta), & \text{if } \phi(\theta) \geq 0 \text{ and } \phi'(\theta) y > 0. \end{cases} \tag{11}$$

It follows from Definition 2.1 that $(\theta - \theta^*)^{\mathrm{T}}(\mathrm{Proj}(\theta, y) - y) \geq 0$, $\theta^* \in \mathbb{R}^n$ holds Lavretsky and Wise (2013). The definition of the projection operator can be generalised to matrices as $\mathrm{Proj}_{\mathrm{m}}(\Theta, Y) = (\mathrm{Proj}(\mathrm{col}_1(\Theta), \mathrm{col}_1(Y)), \ldots, \mathrm{Proj}(\mathrm{col}_m(\Theta), \mathrm{col}_m(Y)))$, where $\Theta \in \mathbb{R}^{n \times m}$, $Y \in \mathbb{R}^{n \times m}$, and $\mathrm{col}_i(\cdot)$ denotes the ith column operator. In this case, $\mathrm{tr}\,[(\Theta - \Theta^*)^{\mathrm{T}}(\mathrm{Proj}_{\mathrm{m}}(\Theta, Y) - Y)] = \sum_{i=1}^{m} [\mathrm{col}_i(\Theta - \Theta^*)^{\mathrm{T}} (\mathrm{Proj}(\mathrm{col}_i(\Theta), \mathrm{col}_i(Y)) - \mathrm{col}_i(Y))] \leq 0$ holds, where $\Theta^* \in \mathbb{R}^{n \times m}$.

3. Nonminimal state space realisation: an overview

In this section, we provide an overview of the nonminimal state-space representation used in Yucelen and Pourboghrat (2009), Albattat et al. (2018) and Yucelen and Haddad (2012) within the context of the problem addressed in this paper. Specifically, this pertains to the dynamics of the follower vehicles, indexed by $i = 1, \ldots, N_{\mathrm{F}}$, for which an equivalent input-output system dynamics representation is derived to facilitate the application of the $(\mathrm{OF})^2\mathrm{AC}$ in the next section. To this end, consider the controllable and observable minimum-phase linear uncertain dynamical model for each follower vehicle $i = 1, \ldots, N_{\mathrm{F}}$, given by

$$\dot{x}_i(t) = Ax_i(t) + Bu_i(t) + Bw_i(t), \quad x_i(0) = x_{0i},\ t \geq 0, \tag{12}$$

$$y_i(t) = Cx_i(t), \tag{13}$$

where $x_i(t) \in \mathbb{R}^n$, $t \geq 0$ is the unknown state vector, $u_i(t) \in \mathbb{R}^m$, $t \geq 0$ is the known control input, $y_i(t) \in \mathbb{R}^l$, $t \geq 0$ is the known system output, and $w_i(t) \in \mathbb{R}^m$, $t \geq 0$ is the unknown input disturbance, with $\|w_i(t)\| \leq w_i^*$ and $\|w_i^{(k)}(t)\| \leq w_i^{(k)*}$, where $Z^{(k)} =$

$\frac{dZ^k}{d^k t}$, $i = 1, \ldots, N_{\mathrm{F}}$, and $k = 1, \ldots, n-1$. Additionally, the system matrices $A \in \mathbb{R}^{n\times n}$, $B \in \mathbb{R}^{n\times m}$, and $C \in \mathbb{R}^{l\times n}$ are known and minimal. An input-output equivalent nonminimal observer canonical state-space model for the system in (12) and (13), from control inputs $u_i(t)$, $t \geq 0$ to system outputs $y_i(t)$, $t \geq 0$, when $l > 1$, is given by Antsaklis and Michel (2006)

$$\dot{x}_{oi}(t) = A_o x_{oi}(t) + B_o u_i(t) + B_o w_i(t),$$
$$x_{oi}(0) = x_{o0i},\ t \geq 0, \tag{14}$$
$$y_i(t) = C_o x_{oi}(t), \tag{15}$$

where $x_{oi}(t) \in \mathbb{R}^{ln}$, $t \geq 0$ is the state vector,

$$A_o = \begin{bmatrix} 0 & I_l & \cdots & 0 \\ \vdots & \ddots & \ddots & \vdots \\ 0 & \cdots & 0 & I_l \\ -a_0 I_l & -a_1 I_l & \cdots & -a_{n-1} I_l \end{bmatrix} \in \mathbb{R}^{ln\times ln}, \tag{16}$$

$$B_o = \begin{bmatrix} CB \\ CAB \\ \vdots \\ CA^{n-1}B \end{bmatrix} \in \mathbb{R}^{ln\times m}, \tag{17}$$

$$C_o = \begin{bmatrix} I_l & \cdots & 0 \end{bmatrix} \in \mathbb{R}^{l\times ln}. \tag{18}$$

Observe that the terms a_k, for $k = 0, 1, \ldots, n-1$, in Equation (16) represent the coefficients of the characteristic polynomial associated with matrix A in Equation (12). Next, define

$$\bar{B}_0 \triangleq C_o(a_1 I_{ln} + a_2 A_o + \cdots + a_{n-2} A_o^{n-3} + a_{n-1} A_o^{n-2} + A_o^{n-1}) B_o, \tag{19}$$
$$\bar{B}_1 \triangleq C_o(a_2 I_{ln} + a_3 A_o + \cdots + a_{n-1} A_o^{n-3} + A_o^{n-2}) B_o, \tag{20}$$
$$\vdots$$
$$\bar{B}_{n-1} \triangleq C_o B_o. \tag{21}$$

An alternative formulation for the input-output equivalent nonminimal controllable state-space representation of (12) and (13) is expressed as

$$\dot{x}_{\mathrm{f}i}(t) = A_{\mathrm{f}} x_{\mathrm{f}i}(t) + B_{\mathrm{f}} u_i(t) + D_{\mathrm{f}} \bar{w}_{\mathrm{f}i}(t),$$
$$x_{\mathrm{f}i}(0) = x_{\mathrm{f}0i},\ t \geq 0, \tag{22}$$
$$y_i(t) = C_{\mathrm{f}} x_{\mathrm{f}i}(t), \tag{23}$$

where $x_{\mathrm{f}i}(t) \in \mathbb{R}^{n_{\mathrm{f}}}$, $t \geq 0$, $n_{\mathrm{f}} \triangleq (m+l)n$, is the known filtered expanded state vector given by

$$x_{\mathrm{f}i}(t) = \left[q_{1i}^{\mathrm{T}}(t), \ldots, q_{ni}^{\mathrm{T}}(t), v_{1i}^{\mathrm{T}}, \ldots, v_{ni}^{\mathrm{T}}\right]^{\mathrm{T}}, \tag{24}$$

where $q_{ki}(t) \triangleq y_{\mathrm{f}i}^{k-1}(t)$, $v_{ki} = u_{\mathrm{f}i}^{k-1}(t)$, $k = 1, 2, \ldots, n$, $z^{(n)} \triangleq \mathrm{d}^n z(t)/\mathrm{d}t^n$, and where $x_{\mathrm{f}i}(t)$ is obtained by filtering $u_i(t)$ and $y_i(t)$ though the filter $\lambda^n/\Lambda(s)$, where

$$\Lambda(s) = (s+\lambda)^n = \sum_{p=0}^{n} \binom{n}{p} s^{n-p}\lambda^p = s^n + n\lambda s^{n-1} + \cdots + \lambda^n, \tag{25}$$

is a monic Hurwitz polynomial of degree n with $\lambda > 0$. In addition,

$$A_{\mathrm{f}} = \begin{bmatrix} 0 & I_l & 0 & \cdots & \cdots & 0 \\ \vdots & & \ddots & & & \vdots \\ 0 & \cdots & 0 & I_l & \cdots & 0 \\ -a_0 I_l & \cdots & \cdots & -a_{n-1} I_l & \cdots & 0 \\ 0 & \cdots & & \cdots & 0 & I_m \\ \vdots & & & & \ddots & \vdots \\ \vdots & & & & \cdots & 0 \\ 0 & \cdots & \cdots & 0 & I_m & 0 \\ \bar{B}_0 & \cdots & \cdots & \bar{B}_{n-1} & 0 & 0 \\ 0 & I_m & 0 & 0 & \cdots & 0 \\ & & \ddots & \vdots & & \vdots \\ & \cdots & 0 & I_m & \cdots & 0 \\ -\lambda^n I_m & \cdots & \cdots & -n\lambda I_m & \cdots & 0 \end{bmatrix} \in \mathbb{R}^{n_{\mathrm{f}}\times n_{\mathrm{f}}}, \tag{26}$$

$$B_{\mathrm{f}} = \begin{bmatrix} 0 & 0 & \cdots & \lambda^n I_m \end{bmatrix}^{\mathrm{T}} \in \mathbb{R}^{n_{\mathrm{f}}\times m}, \tag{27}$$

$$C_{\mathrm{f}} = [-\lambda^{-n}(a_0 I_l + \lambda^n I_l) \quad \cdots \quad \cdots \quad -\lambda^{-n}(a_{n-1} I_l + n\lambda^n I_l) \quad \lambda^{-n}\bar{B}_0 \quad \cdots \quad \cdots \quad \lambda^{-n}\bar{B}_{n-1}] \in \mathbb{R}^{l\times n_{\mathrm{f}}}, \tag{28}$$

$$D_{\mathrm{f}} = \begin{bmatrix} 0 & \cdots & 0 & I_l & 0 & \cdots & 0 & 0 \end{bmatrix}^{\mathrm{T}} \in \mathbb{R}^{n_{\mathrm{f}}\times l}, \tag{29}$$

and

$$\bar{w}_{\mathrm{f}i}(t) = a_1 C_o B_o w_{\mathrm{f}i}(t) + \cdots + a_{n-1} \times [C_o A_o^{n-2} B_o w_{\mathrm{f}i}(t) + \cdots + C_o B_o w_{\mathrm{f}i}^{(n-2)}(t)]$$

$$+ C_o A_o^{n-1} B_o w_{\mathrm{f}i}(t) + \cdots + C_o B_o w_{\mathrm{f}i}^{(n-1)}(t), \quad t \geq 0, \tag{30}$$

where $w_{\mathrm{f}i}(t)$ is derived by passing $w_i(t)$ through the filter $\lambda^n/\Lambda(s)$. Referring to the results presented in Yucelen and Pourboghrat (2009) and Yucelen and Haddad (2012), the dynamics of the ith follower vehicle, described by (12) and (13), are input-output equivalent to the dynamics in (22) and (23) (see Theorem 2.1 in Yucelen and Haddad (2012)).

4. (OF)^{2}AC construction for the follower vehicles

In this section, we present the (OF)^{2}AC method for the follower vehicles. The proposed framework builds upon the observer-free adaptive control concept introduced in Albttat and Yucelen (2025) and is developed under the nonminimal state-space representation described in Section 3. The control architecture consists of two main components: a local cooperative control protocol that utilises relative output information to achieve the containment objective, and a vehicle-level adaptive controller designed to compensate for system uncertainties without requiring state estimation. To enable output-based implementation and improve transient performance, an output emulator reference model is incorporated within the control design. This mechanism provides a compatible reference signal for the adaptive controller while avoiding the need for full state reconstruction. Before proceeding with the controller formulation, we first introduce the leader vehicle dynamics, for $i = 1, \ldots, N_{\mathrm{L}}$, as follows:

$$\dot{x}_{\mathrm{L}i}(t) = A_{\mathrm{L}i} x_{\mathrm{L}i}(t) + B_{\mathrm{L}i} c_i(t), \quad x_{\mathrm{L}i}(0) = x_{\mathrm{L}0i},\ t \geq 0, \tag{31}$$

$$y_{\mathrm{L}i}(t) = C_{\mathrm{L}i} x_{\mathrm{L}i}(t), \tag{32}$$

where $x_{\mathrm{L}i}(t) \in \mathbb{R}^{n_i}$ denotes the state vector of the leader vehicle, and $c_i(t) \in \mathbb{R}^{m_i}$ represents the bounded input command to the leader (i.e. $\|c_i(t)\| \leq c_i^*$) with a bounded rate of change over time (i.e. $\|\dot{c}_i(t)\| \leq \dot{c}^i$). Additionally, $y_{\mathrm{L}i}(t) \in \mathbb{R}^l$ represents the leader vehicle output, while $A_{\mathrm{L}i} \in \mathbb{R}^{n_i \times n_i}$, $B_{\mathrm{L}i} \in \mathbb{R}^{n_i \times m_i}$, and $C_{\mathrm{L}i} \in \mathbb{R}^{l \times n_i}$ are the leader vehicle system matrices, where $(A_{\mathrm{L}i}, B_{\mathrm{L}i}, C_{\mathrm{L}i})$ forms a minimal realisation, and $A_{\mathrm{L}i}$ is Hurwitz. The leader is modeled as a disturbance-free reference generator to provide a well-defined trajectory, while uncertainties are considered only in the follower dynamics to evaluate the robustness of the proposed control strategy.

Next, considering the follower vehicle dynamics under the assumptions and nonminimal representation introduced in Section 3, let d denote the known smallest positive integer r such that the rth Markov parameter of the original follower system (12) and (13), given by $CA^{r-1}B$ is nonzero. From this, it follows from (20)–(21) that

$$\bar{B}_{n-1} = C_o B_o = CB = 0, \tag{33}$$

$$\bar{B}_{n-2} = C_o(a_1 I_{ln} + A_o) B_o = a_1 CB + CAB = 0, \tag{34}$$

$$\vdots$$

$$\bar{B}_{n-d+1} = 0, \tag{35}$$

$$\bar{B}_{n-d} = CA^{d-1}B \neq 0. \tag{36}$$

The first Markov parameter can be expressed as

$$CA^{d-1}B = \bar{B}, \tag{37}$$

where $\bar{B} \in \mathbb{R}^{l \times m}$ is a known matrix, given that A, B, and C are known.

Next, the nonminimal state-space representation in (22) can be decomposed into a set of dynamics similar to the approach in Yucelen and Haddad (2012), as follows:

$$\dot{q}_i(t) = A_0 q_i(t) + B_0 v_{0i}(t) + B_1 \phi_i(t) + D_1 \bar{w}_{\mathrm{f}i}(t), \quad q_i(0) = q_{0i},\ t \geq 0, \tag{38}$$

$$\dot{v}_i(t) = A_v v_i(t) + B_v u_i(t), \quad v_i(0) = v_{0i},\ t \geq 0, \tag{39}$$

where $q_i(t) \triangleq [q_{1i}^{\mathrm{T}}(t), \ldots, q_{ni}^{\mathrm{T}}(t)]^{\mathrm{T}} \in \mathbb{R}^{ln}$, $v_{0i}(t) \triangleq [v_{1i}^{\mathrm{T}}(t), \ldots, v_{(n-d)i}^{\mathrm{T}}(t)]^{\mathrm{T}} \in \mathbb{R}^{m(n-d)}$, $\phi_i(t) \triangleq v_{(n-d+1)i}(t) \in \mathbb{R}^m$, $v_i(t) \triangleq [v_{1i}^{\mathrm{T}}(t), \ldots, v_{ni}^{\mathrm{T}}(t)]^{\mathrm{T}} \in \mathbb{R}^{mn}$, $i = 1, \ldots, N_{\mathrm{F}}$,

$$A_0 \triangleq \begin{bmatrix} 0 & I_l & \cdots & 0 \\ \vdots & \ddots & \ddots & \vdots \\ 0 & \cdots & 0 & I_l \\ -a_0 I_l & -a_1 I_l & \cdots & -a_{n-1} I_l \end{bmatrix} \in \mathbb{R}^{ln \times ln}, \tag{40}$$

$$B_0 \triangleq \begin{bmatrix} 0 & \cdots & 0 \\ \vdots & \ddots & \vdots \\ 0 & \cdots & 0 \\ \bar{B}_o & \cdots & \bar{B}_{n-d-1} \end{bmatrix} \in \mathbb{R}^{ln \times m(n-d)}, \tag{41}$$

$$B_1 \triangleq \begin{bmatrix} 0 & \cdots & 0 & \bar{B}^{\mathrm{T}} \end{bmatrix}^{\mathrm{T}} \in \mathbb{R}^{ln \times m}, \tag{42}$$

$$D_1 \triangleq \begin{bmatrix} 0 & \cdots & 0 & I_l \end{bmatrix}^{\mathrm{T}} \in \mathbb{R}^{ln\times l}, \tag{43}$$

$$A_\nu \triangleq \begin{bmatrix} 0 & I_m & \cdots & 0 \\ \vdots & \ddots & \ddots & \vdots \\ 0 & \cdots & 0 & I_m \\ -\zeta_1 I_m & \cdots & \cdots & -\zeta_n I_m \end{bmatrix} \in \mathbb{R}^{mn\times mn}, \tag{44}$$

and

$$B_\nu \triangleq \begin{bmatrix} 0 & \cdots & 0 & \lambda^n I_m \end{bmatrix}^{\mathrm{T}} \in \mathbb{R}^{mn\times m}, \tag{45}$$

where $\zeta_1 \triangleq \lambda^n, \ldots, \zeta_n \triangleq n\lambda$. Although the input-output transformation introduces augmented states, the resulting computational and communication requirements remain local to each agent and scale independently of the overall network size.

We use a two-stage design (Yucelen & Johnson, 2013) for the virtual control signal $\phi_i(t), t \geq 0$, such that the virtual control can suppress the effect of the unmatched disturbances and stabilise the follower vehicles, and drive the uncertain follower vehicles to the convex hull spanned by the leaders. Then, the actual control signal $u_i(t), t \geq 0$, is designed using the follower second dynamical subsystem in (38). This design process is covered in detail in the following subsections.

4.1. Vehicle-level controller design

We proceed by constructing the virtual controller as

$$\phi_i(t) \triangleq \phi_{\mathrm{n}i}(t) + \phi_{\mathrm{a}i}(t) + \phi_{\mathrm{c}i}(t), \tag{46}$$

where $\phi_{\mathrm{n}i}(t)$ represents the nominal control, $\phi_{\mathrm{a}i}(t)$ denotes the adaptive control, and $\phi_{\mathrm{c}i}(t)$ refers to the cooperative control, which will be elaborated in the subsequent subsection.

The vehicle-level controller is comprised of both the nominal and adaptive controls (with an emphasis on augmenting adaptive control in this context), where the nominal component is specified as

$$\phi_{\mathrm{n}i}(t) \triangleq K_{\mathrm{q}} q_i(t) - K_\nu \nu_{0i}(t), \tag{47}$$

with $K_{\mathrm{q}} \in \mathbb{R}^{m\times ln}$ and $K_\nu \in \mathbb{R}^{m\times m(n-d)}$, ensuring that $A_{\mathrm{m}} \triangleq A_0 + B_1 K_{\mathrm{q}}$ is Hurwitz and $B_0 = B_1 K_\nu$ for some gain matrix K_ν. The presence of a virtual adaptive control $\phi_{\mathrm{a}i}(t)$ for $t \geq 0$ is assured under the following assumption.

Assumption 4.1: *The matrix $\bar{B} \in \mathbb{R}^{l\times m}$ has the dimension satisfying $m \geq l$. In addition, if $m = l$, then $\bar{B}$ is nonsingular (i.e. $\bar{B}\bar{B}^{-1} = \bar{B}^{-1}\bar{B} = I$). Furthermore, if $m > l$, then $\bar{B}$ satisfies $\bar{B}\bar{B}^{\dagger} = I$.*

Using (46), (38) can be written as

$$\begin{aligned} \dot{q}_i(t) &= A_{\mathrm{m}} q_i(t) + B_1\phi_{\mathrm{c}i}(t) + B_1\phi_{\mathrm{a}i}(t) + D_1\bar{w}_{\mathrm{f}i}(t) \\ &= A_{\mathrm{m}} q_i(t) + B_1\phi_{\mathrm{c}i}(t) + B_1\phi_{\mathrm{a}i}(t) + D_1\bar{B}\bar{B}^{\dagger}\bar{w}_{\mathrm{f}i}(t) \\ &= A_{\mathrm{m}} q_i(t) + B_1\phi_{\mathrm{c}i}(t) + B_1\phi_{\mathrm{a}i}(t) + B_1\bar{B}^{\dagger}\bar{w}_{\mathrm{f}i}(t) \\ &= A_{\mathrm{m}} q_i(t) + B_1\phi_{\mathrm{c}i}(t) + B_1\left[\phi_{\mathrm{a}i}(t) + d_{\mathrm{f}i}(t)\right]. \end{aligned} \tag{48}$$

where $d_{\mathrm{f}i}(t) \triangleq \bar{B}^{\dagger}\bar{w}_{\mathrm{f}i}(t)$ is unknown. This transformation recasts the disturbance into a matched form with respect to the virtual control input. Now, consider the ideal reference system given by

$$\dot{q}_{\mathrm{m}i}(t) = A_{\mathrm{m}} q_{\mathrm{m}i}(t) + B_1\phi_{\mathrm{c}i}(t). \tag{49}$$

The error dynamics then follow from the state error vector $e_i(t) \triangleq q_i(t) - q_{\mathrm{m}i}(t)$, (48), and (49) as

$$\dot{e}_i(t) = A_{\mathrm{m}} e_i(t) + B_1\left[\phi_{\mathrm{a}i}(t) + d_{\mathrm{f}i}(t)\right]. \tag{50}$$

Next, let the virtual adaptive control law of the vehicle $i, i = 1, \ldots, N_{\mathrm{F}}$, be given by

$$\phi_{\mathrm{a}i}(t) \triangleq -\hat{d}_{\mathrm{f}i}(t), \tag{51}$$

where, $\hat{d}_{\mathrm{f}i}(t) \in \mathbb{R}^m$ is the estimate of $d_{\mathrm{f}i}(t)$ satisfying the update law

$$\dot{\hat{d}}_{\mathrm{f}i}(t) = \Gamma\,\mathrm{Proj}\left[\hat{d}_{\mathrm{f}i}(t), \left(e_i^{\mathrm{T}}(t)PB_1\right)^{\mathrm{T}}\right], \quad \hat{d}_{\mathrm{f}i}(0) = \hat{d}_{\mathrm{f}0i} \tag{52}$$

where $\Gamma = \gamma I_m \in \mathbb{R}^{m\times m}$, with $\gamma \in \mathbb{R}_+$, is a positive-definite learning rate matrix, Proj represents a projection operator (Pomet & Praly, 1992), used to ensure the uniform boundedness of the weight update error, and $P \in \mathbb{R}^{ln\times ln}$ is a positive definite solution of the Lyapunov equation

$$0 = A_{\mathrm{m}}^{\mathrm{T}} P + PA_{\mathrm{m}} + R, \tag{53}$$

where $R \in \mathbb{R}^{ln\times ln}$ is a positive definite matrix. The adaptive component of the virtual control is designed to compensate for the effect of uncertainties and disturbances in the input-output channel. Although the disturbance appears as unmatched in the nonminimal

realisation, the proposed decomposition and projection using Assumption 4.1 reformulate its effect into an equivalent matched disturbance acting through the virtual control channel. This enables the adaptive law to attenuate the impact of the disturbance in real time based on the tracking error signal, without requiring state estimation. It then follows that (50) can be written using (51) as

$$\dot{e}_i(t) = A_{\mathrm{m}} e_i(t) - B_1 \tilde{d}_{\mathrm{f}i}(t), \tag{54}$$

where $\tilde{d}_{\mathrm{f}i}(t) \triangleq \hat{d}_{\mathrm{f}i}(t) - d_{\mathrm{f}i}(t)$ is the weight update error.

4.2. Output emulator-based adaptive control construction

We present the output emulator-based adaptive control framework, inspired by the state emulator-based adaptive control approaches in Lavretsky et al. (2010), Gibson et al. (2012b), Gibson et al. (2012a) and Albattat, Gruenwald, et al. (2017). While the ideal reference model in (49) provides a target trajectory for tracking, its direct use may introduce high-frequency oscillations in the control signal due to the lack of damping in the reference dynamics. This issue becomes more pronounced in the presence of uncertainties and adaptive updates. To address this limitation, a modified reference system, referred to as the output emulator, is introduced. The output emulator incorporates a correction term based on the measurable signal $q_i(t)$, improving transient performance while remaining consistent with the observer-free control framework, where full state reconstruction is not available. This modification preserves generality, as the standard reference model in (49) is recovered when $L = 0$. Consider the (modified) reference system so-called the output emulator given by

$$\dot{q}_{\mathrm{e}i}(t) = A_{\mathrm{m}} q_{\mathrm{e}i}(t) + B_1 \phi_{ci}(t) + L(q_i(t) - q_{\mathrm{e}i}(t)). \tag{55}$$

where $L \in \mathbb{R}^{ln\times ln} \cap \mathbb{S}^{ln\times ln}$ is the output emulator gain. The additional feedback term $L(q_i(t) - q_{\mathrm{e}i}(t))$ introduces a stable error feedback mechanism that effectively injects damping into the reference dynamics, thereby attenuating high-frequency components and improving the smoothness of the resulting control signal. Letting $\tilde{q}_i(t) \triangleq q_{\mathrm{e}i}(t) - q_{\mathrm{m}i}(t) \in \mathbb{R}^{ln}$, the reference system error dynamics capturing the difference between the ideal reference model (49) and the output emulator-based (modified) reference model (55) is given by

$$\dot{\tilde{q}}_i(t) = A_{\mathrm{m}} \tilde{q}_i(t) + L(q_i(t) - q_{\mathrm{e}i}(t)), \quad \tilde{q}_i(0) = \tilde{q}_{i0}. \tag{56}$$

In addition, letting $e_{\mathrm{e}i}(t) \triangleq q_i(t) - q_{\mathrm{e}i}(t)$ to denote the system output error vector, the output emulator-based system error dynamics through (48) and (55) given by

$$\begin{aligned} \dot{e}_{\mathrm{e}i}(t) &= A_L e_{\mathrm{e}i}(t) + B_1 \left[\phi_{\mathrm{a}i}(t) + d_{\mathrm{f}i}(t)\right], \\ e_{\mathrm{e}i}(0) &= e_{\mathrm{e}i0}, \end{aligned} \tag{57}$$

where $A_L \triangleq A_{\mathrm{m}} - L \in \mathbb{R}^{ln\times ln}$ is Hurwitz for an appropriately chosen output emulator gain L (for instance, A_L is Hurwitz with $L = \kappa I_{ln}$, where $\kappa \in \mathbb{R}^+$, given that A_{m} is Hurwitz). Setting $L = 0$ recovers the standard reference model in (49) as a special case. Furthermore, let the virtual adaptive control law for vehicle i, where $i = 1, \ldots, N_{\mathrm{F}}$, be defined by (51), with $\hat{d}_{\mathrm{f}i}(t)$ adhering to a new weight update law.

$$\begin{aligned} \dot{\hat{d}}_{\mathrm{f}i}(t) &= \Gamma \mathrm{Proj}\left[\hat{d}_{\mathrm{f}i}(t), \left(e_{\mathrm{e}i}^{\mathrm{T}}(t)\tilde{P}B_1\right)^{\mathrm{T}}\right], \\ \hat{d}_{\mathrm{f}i}(0) &= \hat{d}_{\mathrm{f}0i}, \end{aligned} \tag{58}$$

where $\tilde{P} \in \mathbb{R}^{ln\times ln}$ is a positive definite solution of the Lyapunov equation

$$0 = A_{\mathrm{L}}^{\mathrm{T}}\tilde{P} + \tilde{P}A_{\mathrm{L}} + \tilde{R}, \tag{59}$$

where $\tilde{R} \in \mathbb{R}^{ln\times ln}$ is a positive definite matrix. Note that using (51) with (58), (57) can be written as

$$\dot{e}_{\mathrm{e}i}(t) = A_L e_{\mathrm{e}i}(t) - B_1 \tilde{d}_{\mathrm{f}i}(t), \quad e_{\mathrm{e}i}(0) = e_{\mathrm{e}i0}, \tag{60}$$

where $\tilde{d}_{\mathrm{f}i}(t)$ is weight update error and weight update error dynamics is given by

$$\dot{\tilde{d}}_{\mathrm{f}i}(t) = \Gamma \mathrm{Proj}\left[\hat{d}_{\mathrm{f}i}(t), \left(e_{\mathrm{e}i}^{\mathrm{T}}(t)\tilde{P}B_1\right)^{\mathrm{T}}\right] - \dot{d}_{\mathrm{f}i}(t). \tag{61}$$

4.3. Local cooperative control design

For the virtual control framework, let $\tilde{y}(t) \triangleq [y_{\mathrm{L}}^T(t), y_{\mathrm{f}}^T(t)]^T \in \mathbb{R}^{(N_{\mathrm{L}}\times N_{\mathrm{F}})l}$ represent the vector associated with the graph $\mathcal{G}$, where $y_{\mathrm{L}}^T(t) \triangleq [y_{\mathrm{L}1}^T(t), \ldots, y_{\mathrm{L}N_{\mathrm{L}}}^T(t)]^T \in \mathbb{R}^{N_{\mathrm{L}}l}$ denotes the first N_{L} nodes, which correspond to the aggregated output vector of the leader nodes,

and $y_{\mathrm{f}}^{T}(t) \triangleq [y_{\mathrm{f}1}^{T}(t), \ldots, y_{\mathrm{f}N_{\mathrm{F}}}^{T}(t)]^{T} \in \mathbb{R}^{N_{\mathrm{F}}l}$ represents the last N_{F} nodes, corresponding to the aggregated output vector of the follower vehicles. Next, for each follower vehicle, consider the local cooperative controller that processes the relative output measurements from neighbouring vehicles. This is expressed in terms of $y_{\mathrm{f}i}(t)$ for $i = 1, \ldots, N_{\mathrm{F}}$, and $y_{\mathrm{L}i}(t)$ for $i = 1, \ldots, N_{\mathrm{L}}$, as detailed in Yucelen and Johnson (2013).

$$\phi_{ci}(t) = K_c \left[-\sum_{i\sim j} \left(\tilde{y}_i(t) - \tilde{y}_j(t)\right) + \theta_i(t) \right], \quad (62)$$

$$\begin{aligned} \dot{\theta}_i(t) &= \delta \left[-\sum_{i\sim j} \left(\tilde{y}_i(t) - \tilde{y}_j(t)\right) \right. \\ &\quad \left. - \zeta \left(\theta_i(t) - \nu_i(t)\right) \right], \\ \theta_i(0) &= \theta_{i0}, \end{aligned} \quad (63)$$

$$\dot{\nu}_i(t) = \eta \left(\theta_i(t) - \nu_i(t)\right), \quad \nu_i(0) = \nu_{i0}, \quad (64)$$

where $K_c \in \mathbb{R}^{m\times l}$ represents the gain matrix, $\theta_i(t) \in \mathbb{R}^l$ denotes the integrator state, $\nu_i(t) \in \mathbb{R}^l$ is the filter state, $\delta \in \mathbb{R}+$ signifies the integrator gain, $\zeta \in \mathbb{R}+$ represents a modification gain, and $\eta \in \mathbb{R}+$ is the filter gain. Subsequently, by applying the local cooperative controller defined in (62), (63), and (64) to the output emulator reference system described by (55) yields

$$\begin{aligned} \dot{q}_{ei}(t) &= A_{\mathrm{m}} q_{ei}(t) - B_1 K_c \sum_{i\sim j} \left(\tilde{y}_i(t) - \tilde{y}_j(t)\right) \\ &\quad + B_1 K_c \theta_i(t) + L \left(q_i(t) - q_{ei}(t)\right). \end{aligned} \quad (65)$$

Letting $q_{\mathrm{e}}(t) \triangleq [q_{\mathrm{e}1}^{\mathrm{T}}(t), \ldots, q_{\mathrm{e}N_{\mathrm{F}}}^{\mathrm{T}}(t)]^{\mathrm{T}} \in \mathbb{R}^{N_{\mathrm{F}}ln}$, $q(t) \triangleq [q_1^{\mathrm{T}}(t), \ldots, q_{N_{\mathrm{F}}}^{\mathrm{T}}(t)]^{\mathrm{T}} \in \mathbb{R}^{N_{\mathrm{F}}ln}$, $e_{\mathrm{e}}(t) = q(t) - q_{\mathrm{e}}(t) \in \mathbb{R}^{N_{\mathrm{F}}ln}$, $\theta(t) \triangleq [\theta_1^{\mathrm{T}}(t), \ldots, \theta_{N_{\mathrm{F}}}^{\mathrm{T}}(t)]^{\mathrm{T}} \in \mathbb{R}^{N_{\mathrm{F}}l}$, $\nu(t) \triangleq [\nu_1^{\mathrm{T}}(t), \ldots, \nu_{N_{\mathrm{F}}}^{\mathrm{T}}(t)]^{\mathrm{T}} \in \mathbb{R}^{N_{\mathrm{F}}l}$, and

$$y_{\mathrm{f}i}(t) = C_q q_i(t), \quad (66)$$

where $C_q \triangleq [I_l, \ldots, 0] \in \mathbb{R}^{l\times ln}$, the output emulator reference system described in (55), when subject to the local cooperative controller given by (62), (63), and (64), can be expressed at the multivehicle system level as

$$\begin{aligned} \dot{q}_{\mathrm{e}}(t) &= (I_{N_{\mathrm{F}}} \otimes A_{\mathrm{m}}) q_{\mathrm{e}}(t) - (F(\mathcal{G}) \otimes B_1 K_c) y_{\mathrm{f}}(t) \\ &\quad - (G(\mathcal{G}) \otimes B_1 K_c) y_{\mathrm{L}}(t) + (I_{N_{\mathrm{F}}} \otimes B1 K_c)\theta(t) \\ &\quad + (I_{N_{\mathrm{F}}} \otimes L) e_{\mathrm{e}}(t) \\ &= [I_{N_{\mathrm{F}}} \otimes A_{\mathrm{m}} - F(\mathcal{G}) \otimes B_1 K_c C_q] q_{\mathrm{e}}(t) \\ &\quad - (F(\mathcal{G}) \otimes B_1 K_c C_q \\ &\quad - I_{N_{\mathrm{F}}} \otimes L) e_{\mathrm{e}}(t) - (G(\mathcal{G}) \otimes B_1 K_c) y_{\mathrm{L}}(t) \\ &\quad + (I_{N_{\mathrm{F}}} \otimes B_1 K_c)\theta(t), \quad q_{\mathrm{e}}(0) = q_{\mathrm{e}0}, \end{aligned} \quad (67)$$

$$\begin{aligned} \dot{\theta}(t) &= -\delta(F(\mathcal{G}) \otimes I_l) y_{\mathrm{f}}(t) - \delta(G(\mathcal{G}) \otimes I_l) y_{\mathrm{L}}(t) \\ &\quad - \delta\zeta \left(\theta(t) - \nu(t)\right) \\ &= -\delta(F(\mathcal{G}) \otimes C_q) q_{\mathrm{e}}(t) - \delta(F(\mathcal{G}) \otimes C_q) e_{\mathrm{e}}(t) \\ &\quad - \delta(G(\mathcal{G}) \otimes I_l) y_{\mathrm{L}}(t) \\ &\quad - \delta\zeta \left(\theta(t) - \nu(t)\right), \quad \theta(0) = \theta_0, \end{aligned} \quad (68)$$

$$\dot{\nu}(t) = \eta \left(\theta(t) - \nu(t)\right), \quad \nu(0) = \nu_0. \quad (69)$$

Now, with $\xi_{\mathrm{e}}(t) \triangleq [q_{\mathrm{e}}^{\mathrm{T}}(t),\ \theta^{\mathrm{T}}(t),\ \nu^{\mathrm{T}}(t)]^{\mathrm{T}} \in \mathbb{R}^{n_\xi}$, $n_\xi \triangleq N_{\mathrm{F}}(ln + 2l)$, $A_\xi(\mathcal{G}) \triangleq I_{N_{\mathrm{F}}} \otimes A_{\mathrm{m}} - F(\mathcal{G}) \otimes B_1 K_c C_q \in \mathbb{R}^{N_{\mathrm{F}}ln\times N_{\mathrm{F}}ln}$, (67), (68), and (69) can be written in compact form as

$$\begin{aligned} \dot{\xi}_{\mathrm{e}}(t) &= \mathcal{A}(\mathcal{G})\xi_{\mathrm{e}}(t) + \mathcal{B}(\mathcal{G}) y_{\mathrm{L}}(t) + \mathcal{E}_{\mathrm{e}}(\mathcal{G}) e_{\mathrm{e}}(t), \\ \xi_{\mathrm{e}}(0) &= \xi_{\mathrm{e}0}, \end{aligned} \quad (70)$$

where

$$\begin{aligned} \mathcal{A}(\mathcal{G}) &= \begin{bmatrix} A_\xi(\mathcal{G}) & I_{N_{\mathrm{F}}} \otimes B_1 K_c & 0 \\ -\delta(F(\mathcal{G}) \otimes C_q) & -\delta\zeta I_{N_{\mathrm{F}}l} & \delta\zeta I_{N_{\mathrm{F}}l} \\ 0 & \eta I_{N_{\mathrm{F}}l} & -\eta I_{N_{\mathrm{F}}l} \end{bmatrix} \\ &\in \mathbb{R}^{n_\xi \times n_\xi}, \end{aligned} \quad (71)$$

$$\mathcal{B}(\mathcal{G}) = \begin{bmatrix} -G(\mathcal{G}) \otimes B_1 K_c \\ -\delta(G(\mathcal{G}) \otimes I_l) \\ 0 \end{bmatrix} \in \mathbb{R}^{n_\xi \times N_{\mathrm{F}}ln}, \quad (72)$$

$$\begin{aligned} \mathcal{E}_{\mathrm{e}}(\mathcal{G}) &= \begin{bmatrix} -(F(\mathcal{G}) \otimes B_1 K_c C_q) + (I_{N_{\mathrm{F}}} \otimes L) \\ -\delta(F(\mathcal{G}) \otimes C_q) \\ 0 \end{bmatrix} \\ &\in \mathbb{R}^{n_\xi \times N_{\mathrm{F}}ln}. \end{aligned} \quad (73)$$

The goal of the output emulator-based observer-free vehicle-level controller discussed in the preceding section is to stabilise the dynamics of the uncertain follower vehicles. Additionally, the purpose of the local cooperative controller, as detailed in this section and based on Yucelen and Johnson (2013), is to address the containment problem. To achieve this, it is necessary to first verify that the solution $\xi(t)$ to (70) is $\mathcal{L}_\infty$ stable (Khalil, 1996). Specifically, for every bounded input $y_{\mathrm{L}}(t)$ and $e_{\mathrm{e}}(t)$, the solution $\xi(t)$ must also be bounded. Since $y_{\mathrm{L}}(t)$ is bounded (as all $A_{\mathrm{L}i}$ for $i = 1, \ldots, N_{\mathrm{L}}$ are Hurwitz), and it will be demonstrated later that $e_{\mathrm{e}}(t)$ either approaches zero as $t \to \infty$ or remains bounded, it follows that to ensure $\mathcal{L}_\infty$ stability of (70), the matrix

$\mathcal{A}(\mathcal{G})$ must be Hurwitz. The desired $\mathcal{L}_\infty$ stability of the system can be equivalently assessed by

$$\dot{\bar{\xi}}(t) = \mathcal{A}(\mathcal{G})\bar{\xi}(t) + \mathcal{B}(\mathcal{G})y_{\mathrm{L}}(t), \quad \bar{\xi}(0) = \bar{\xi}_0, \quad (74)$$

where $\bar{\xi}(t) \in \mathbb{R}^{n_\xi}$. A necessary and sufficient condition satisfying this requirement is given in the following remark.

Remark 4.1: Similar to the results in Fax and Murray (2004), Ma and Zhang (2010) and Yucelen and Johnson (2013), let $\mu_i \in \mathrm{spec}(F(\mathcal{G})), i = 1, \ldots, N_{\mathrm{F}}$. If the matrix storing known parts of the system dynamics as well as the controller parameters

$$\mathcal{U}_{\mathcal{A}(\mathcal{G})i} = \begin{bmatrix} A_{\mathrm{m}} - \mu_i B_1 K_{\mathrm{c}} C_q & B_1 K_{\mathrm{c}} & 0 \\ -\mu_i \delta C_q & -\delta\zeta I_l & \delta\zeta I_l \\ 0 & \eta I_l & \eta I_l \end{bmatrix} \in \mathbb{R}^{(ln+2l)\times(ln+2l)}, \quad (75)$$

is Hurwitz for $i = 1, \ldots, N_{\mathrm{F}}$, then $\mathcal{A}(\mathcal{G})$ in (71) is Hurwitz.

It is important to note that (75) can be rendered Hurwitz for $i = 1, \ldots, N_{\mathrm{F}}$ through an appropriate selection of the design parameters K_{c}, δ, ζ, and η. This, in turn, ensures that the system described by (70), together with the leader dynamics given by (31) and (32), is $\mathcal{L}_\infty$ stable (for instance, refer to Corollary 6.1 in Yucelen and Johnson (2013)).

4.4. Actual control construction

We construct the actual control signal $u_i(t)$, $t > 0$, for the $(\mathrm{OF})^2\mathrm{AC}$ using the system dynamics in (39) as

$$\begin{aligned} u_i(t) = {} & \dot{\nu}_i(t) + \zeta_n \nu_{ni} + \zeta_{n-1}\nu_{(n-1)i} + \zeta_{n-2}\nu_{(n-2)i} \\ & + \cdots + \zeta_{n-d+2}\nu_{(n-d+2)i} + \zeta_{n-d+1}\nu_{(n-d+1)i} \\ & + \zeta_{n-d}\nu_{(n-d)i} + \cdots + \zeta_2\nu_{2i} + \zeta_1\nu_{1i}, \quad t \geq 0. \end{aligned} \quad (76)$$

Using $\phi(t), t \geq 0$ given by (46), it then follows from (76) that Yucelen and Haddad (2012) and Albattat et al. (2018)

$$\begin{aligned} u_i(t) = {} & \phi_i^{(d)}(t) + \zeta_n \phi_i^{(d-1)}(t) + \zeta_{n-1}\phi_i^{(d-2)}(t) \\ & + \cdots + \zeta_{n-d+2}\dot{\phi}_i(t) + \zeta_{n-d+1}\phi_i(t) \\ & + \zeta_{n-d}\int_0^t \phi_i(\sigma_1)\mathrm{d}\sigma_1 + \cdots \\ & + \zeta_2 \left(\int_0^t \cdots \int_0^t \left(\int_0^t \phi_i(\sigma_1)\mathrm{d}\sigma_1 \right) \right. \\ & \left. \mathrm{d}\sigma_2 \cdots \mathrm{d}\sigma_{n-d-1} \right) \\ & + \zeta_1 \left(\int_0^t \cdots \int_0^t \left(\int_0^t \phi_i(\sigma_1)\mathrm{d}\sigma_1 \right) \right. \\ & \left. \mathrm{d}\sigma_2 \cdots \mathrm{d}\sigma_{n-d} \right), \\ & t \geq 0. \end{aligned} \quad (77)$$

5. Stability analysis

To examine the stability of the overall multivehicle system, let $\tilde{w}(t) \triangleq [\tilde{d}_{\mathrm{f}1}^T(t), \ldots, \tilde{d}_{\mathrm{f}N_{\mathrm{F}}}^T(t)]^T \in \mathbb{R}^{N_{\mathrm{F}}m}$ and $\dot{w}(t) \triangleq [\dot{d}_{\mathrm{f}1}^T(t), \ldots, \dot{d}_{\mathrm{f}N_{\mathrm{F}}}^T(t)]^T \in \mathbb{R}^{N_{\mathrm{F}}m}$. The following part of this section focuses on the stability analysis. Additionally, consider

$$\dot{\tilde{\xi}}(t) = \mathcal{A}(\mathcal{G})\tilde{\xi}(t) + \mathcal{E}_{\mathrm{e}}(\mathcal{G})e_{\mathrm{e}}(t), \quad \tilde{\xi}(0) = \tilde{\xi}_0, \quad (78)$$

where $\tilde{\xi}(t) \triangleq \xi(t) - \bar{\xi}(t), \tilde{\xi}(t) \in \mathbb{R}^{n_\xi}$.

Theorem 5.1: *Consider a multivehicle system consisting of N_{F} uncertain vehicles with the dynamics given by (38), for $i = 1, \ldots, N_{\mathrm{F}}$, with time-varying input disturbance, subject to Assumption 4.1, the ideal reference model given by (49), the output emulator given by (55), and the virtual vehicle-level controller given by (46), (47), (51), and (52). In addition, let the virtual local cooperative control for vehicle $i = 1, \ldots, N_{\mathrm{F}}$, be given by (62), (63), and (64), such that (71) is Hurwitz. Then, the solution $(e_{\mathrm{e}}(t), \tilde{\xi}(t), \tilde{w}(t), \tilde{q}(t))$ is uniformly ultimately bounded for all initial conditions.*

Proof: To show uniform ultimate boundedness of the solution $(e_{\mathrm{e}}(t), \tilde{\xi}(t), \tilde{w}(t), \tilde{q}(t))$ for all $(e_{\mathrm{e}}(0), \tilde{\xi}(0), \tilde{w}(0), \tilde{q}(0)) \in \mathbb{R}^{N_{\mathrm{F}}ln} \times \mathbb{R}^{n_\xi} \times \mathbb{R}^{N_{\mathrm{F}}m}$ and $t \in \overline{\mathbb{R}}_+$, first consider

$$\begin{aligned} \mathcal{V}_{1i}(e_{ei}(t), \tilde{d}_{\mathrm{f}i}(t), \tilde{q}_i(t)) = {} & e_{ei}^{\mathrm{T}}(t)Pe_{ei}(t) \\ & + \tilde{d}_{\mathrm{f}i}^{\mathrm{T}}(t)\Gamma^{-1}\tilde{d}_{\mathrm{f}i}(t) + \beta\tilde{q}_i^{\mathrm{T}}(t)\tilde{P}\tilde{q}_i(t), \end{aligned} \quad (79)$$

and note that $\mathcal{V}_{1i}(0,0,0) = 0$, $\mathcal{V}_{1i}(e_{ei}(t), \tilde{d}_{\mathrm{f}i}(t), \tilde{q}_i(t)) > 0$ for all $(e_{ei}(t), \tilde{d}_{\mathrm{f}i}(t), \tilde{q}_i(t)) \neq (0,0,0)$, and $\mathcal{V}_{1i}(e_{ei}(t), \tilde{d}_{\mathrm{f}i}(t), \tilde{q}_i(t))$ is radially unbounded. The time derivative of (79) is then given by

$$\begin{aligned} \dot{\mathcal{V}}_{1i}(\cdot) = {} & 2e_{ei}^{\mathrm{T}}(t)P\left(A_{\mathrm{m}}e_{ei}(t) - B_1\tilde{d}_{\mathrm{f}i}(t)\right) \\ & + 2\tilde{d}_{\mathrm{f}}^{\mathrm{T}}(t)\Gamma^{-1} \end{aligned}$$

$$\times \left(\Gamma \mathrm{Proj}\left[\hat{d}_{\mathrm{f}i}(t), \left(e_{\mathrm{e}i}^{\mathrm{T}}(t)PB_1\right)^{\mathrm{T}}\right] - \dot{d}_{\mathrm{f}i}(t)\right)$$
$$+ \beta \tilde{q}_i^{\mathrm{T}}(t)\tilde{P}\left(A_{\mathrm{m}}\tilde{q}_i(t) + L(q_i(t) - q_{\mathrm{e}i}(t))\right)$$
$$\leq -e_{\mathrm{e}i}^{\mathrm{T}}(t)Re_{\mathrm{e}i}(t) - 2\tilde{d}_{\mathrm{f}i}^{\mathrm{T}}(t)\Gamma^{-1}\dot{d}_{\mathrm{f}i}(t)$$
$$- \beta \tilde{q}_i^{\mathrm{T}}(t)\tilde{R}\tilde{q}_i(t) - 2\beta \tilde{q}_i^{\mathrm{T}}(t)Le_{\mathrm{e}i}(t). \tag{80}$$

Now, by introducing

$$\mathcal{V}_1(e_{\mathrm{e}}(t), \tilde{w}(t), \tilde{q}(t)) = \sum_{i=1}^{N_{\mathrm{F}}} \mathcal{V}_{1i}(e_{\mathrm{e}i}(t), \tilde{d}_{\mathrm{f}i}(t), \tilde{q}_i(t)), \tag{81}$$

it follows from (80) that

$$\dot{\mathcal{V}}_1(\cdot) \leq -e_{\mathrm{e}}^{\mathrm{T}}(t)(I_{N_{\mathrm{F}}} \otimes R)e_{\mathrm{e}}(t)$$
$$- 2\tilde{w}^{\mathrm{T}}(t)(I_{N_{\mathrm{F}}} \otimes \Gamma^{-1})\dot{w}(t)$$
$$- \tilde{q}^{\mathrm{T}}(t)(I_{N_{\mathrm{F}}} \otimes \beta\tilde{R})\tilde{q}(t)$$
$$- 2\tilde{q}^{\mathrm{T}}(t)(I_{N_{\mathrm{F}}} \otimes \beta L)e_{\mathrm{e}}(t). \tag{82}$$

Next, consider

$$\mathcal{V}_2(\tilde{\xi}(t)) = \tilde{\xi}^{\mathrm{T}}(t)\mathcal{P}\tilde{\xi}(t), \tag{83}$$

where since $\mathcal{A}(\mathcal{G})$ is Hurwitz, it follows from converse Lyapunov theory (Haddad & Chellaboina, 2008) that there is exists a unique $\mathcal{P} \in \mathbb{R}_+^{n_\xi \times n_\xi} \cap \mathbb{S}_+^{n_\xi \times n_\xi}$ satisfying

$$0 = \mathcal{A}(\mathcal{G})^{\mathrm{T}}\mathcal{P} + \mathcal{P}\mathcal{A}(\mathcal{G}) + \mathcal{R}, \tag{84}$$

with given $\mathcal{R} \in \mathbb{R}_+^{n_\xi \times n_\xi} \cap \mathbb{S}_+^{n_\xi \times n_\xi}$. Furthermore, note that $\mathcal{V}_2(0) = 0$, $\mathcal{V}_2(\tilde{\xi}(t)) > 0$ for all $\tilde{\xi}(t) \neq 0$, and $\mathcal{V}_2(\tilde{\xi}(t))$ is radially unbounded. Differentiation of (83) yields

$$\dot{\mathcal{V}}_2(\tilde{\xi}(t)) = 2\tilde{\xi}^{\mathrm{T}}(t)\mathcal{P}\left(\mathcal{A}(\mathcal{G})\tilde{\xi}(t) + \mathcal{E}_{\mathrm{e}}(\mathcal{G})e_{\mathrm{e}}(t)\right)$$
$$= -\tilde{\xi}^{\mathrm{T}}(t)\mathcal{R}\tilde{\xi}(t) + 2\tilde{\xi}^{\mathrm{T}}(t)\mathcal{P}\mathcal{E}_{\mathrm{e}}(\mathcal{G})e_{\mathrm{e}}(t). \tag{85}$$

Applying Young's inequality (Bernstein, 2009) to the last term of (85) gives

$$2\tilde{\xi}^{\mathrm{T}}(t)\mathcal{P}\mathcal{E}_{\mathrm{e}}(\mathcal{G})e_{\mathrm{e}}(t) \leq \frac{1}{k}e_{\mathrm{e}}^{\mathrm{T}}(t)\mathcal{E}_{\mathrm{e}}(\mathcal{G})^{\mathrm{T}}\mathcal{P}^2\mathcal{E}_{\mathrm{e}}(\mathcal{G})e_{\mathrm{e}}(t)$$
$$+ k\tilde{\xi}^{\mathrm{T}}(t)\tilde{\xi}(t), \tag{86}$$

where $k \in \mathbb{R}_+$ is an arbitrary constant that satisfies $\mathcal{R} - kI_{n_\xi} > 0$. Now, using (86) in (85) yields

$$\dot{\mathcal{V}}_2(\tilde{\xi}(t)) \leq -\tilde{\xi}^{\mathrm{T}}(t)\left(\mathcal{R} - kI_{n_\xi}\right)\tilde{\xi}(t)$$
$$+ \frac{1}{k}e_{\mathrm{e}}^{\mathrm{T}}(t)\mathcal{E}_{\mathrm{e}}(\mathcal{G})^{\mathrm{T}}\mathcal{P}^2\mathcal{E}_{\mathrm{e}}(\mathcal{G})e_{\mathrm{e}}(t). \tag{87}$$

Consider now, the Lyapunov function candidate using (81) and (83) as

$$\mathcal{V}_{\mathrm{s}}(e_{\mathrm{e}}(t), \tilde{\xi}(t), \tilde{w}(t), \tilde{q}(t)) = \mathcal{V}_1(e_{\mathrm{e}}(t), \tilde{w}(t), \tilde{q}(t))$$
$$+ \alpha\mathcal{V}_2(\tilde{\xi}(t)), \tag{88}$$

where $\alpha \triangleq k\tilde{\alpha} \in \mathbb{R}_+$ satisfies $I_{N_{\mathrm{F}}} \otimes R - \tilde{\alpha}\mathcal{E}_{\mathrm{e}}(\mathcal{G})^{\mathrm{T}}\mathcal{P}^2\mathcal{E}_{\mathrm{e}}(\mathcal{G}) > 0$. Differentiating (88) along (54), (61), and (78), and defining $\mathcal{Q}_1 \triangleq I_{N_{\mathrm{F}}} \otimes R - \tilde{\alpha}\mathcal{E}_{\mathrm{e}}(\mathcal{G})^{\mathrm{T}}\mathcal{P}^2\mathcal{E}_{\mathrm{e}}(\mathcal{G}) > 0$ and $\mathcal{Q}_2 \triangleq \alpha(\mathcal{R} - kI_{n_\xi}) > 0$, it follows from (82) and (87) that

$$\dot{\mathcal{V}}_{\mathrm{s}}(\cdot) \leq -e_{\mathrm{e}}^{\mathrm{T}}(t)\mathcal{Q}_1e_{\mathrm{e}}(t) - \tilde{\xi}^{\mathrm{T}}(t)\mathcal{Q}_2\tilde{\xi}(t) - 2\tilde{w}^{\mathrm{T}}(t)$$
$$\times (I_{N_{\mathrm{F}}} \otimes \Gamma^{-1})\dot{w}(t) - \tilde{q}^{\mathrm{T}}(t)(I_{N_{\mathrm{F}}} \otimes \beta\tilde{R})\tilde{q}(t)$$
$$- 2\tilde{q}^{\mathrm{T}}(t)(I_{N_{\mathrm{F}}} \otimes \beta L)e_{\mathrm{e}}(t)$$
$$\leq -\lambda_{\min}(\mathcal{Q}_1)\|e_{\mathrm{e}}(t)\|^2 - \lambda_{\min}(\mathcal{Q}_2)\|\tilde{\xi}(t)\|^2$$
$$+ 2\|\tilde{w}(t)\|\|(I_{N_{\mathrm{F}}} \otimes \Gamma^{-1})\|_{\mathrm{F}}\|\dot{w}(t)\|$$
$$- \lambda_{\min}\left(I_{N_{\mathrm{F}}} \otimes \beta\tilde{R}\right)\|\tilde{q}(t)\|^2$$
$$+ \|\tilde{q}(t)\|\|\left(I_{N_{\mathrm{F}}} \otimes \beta L\right)\|_{\mathrm{F}}\|e_{\mathrm{e}}(t)\|. \tag{89}$$

Applying again Young's inequality to the last term of (89) gives

$$\|\tilde{q}(t)\|\|\left(I_{N_{\mathrm{F}}} \otimes \beta L\right)\|_{\mathrm{F}}\|e_{\mathrm{e}}(t)\|$$
$$\leq \|\left(I_{N_{\mathrm{F}}} \otimes k_2I_{ln}\right)\|_{\mathrm{F}}\|\tilde{q}(t)\|^2$$
$$+ \|\left(I_{N_{\mathrm{F}}} \otimes \frac{1}{k_2}\beta L\right)\|_{\mathrm{F}}\|e_{\mathrm{e}}(t)\|^2, \tag{90}$$

where $k_2 \in \mathbb{R}_+$ is an arbitrary constant that satisfies the definitions $\mathcal{Q}_3 \triangleq \lambda_{\min}(\mathcal{Q}_1) - \|(I_{N_{\mathrm{F}}} \otimes \frac{1}{k_2}\beta L)\|_{\mathrm{F}} - \|(I_{N_{\mathrm{F}}} \otimes k_2I_{ln})\|_{\mathrm{F}} > 0$ and $\mathcal{Q}_5 \triangleq \lambda_{\min}(I_{N_{\mathrm{F}}} \otimes \beta\tilde{R}) - \|(I_{N_{\mathrm{F}}} \otimes k_2I_{ln})\|_{\mathrm{F}} > 0$ with suitable β. Now, using (90) in (89) yields

$$\dot{\mathcal{V}}_{\mathrm{s}}(\cdot) \leq -\mathcal{Q}_3\|e_{\mathrm{e}}(t)\|^2 - \mathcal{Q}_4\|\tilde{\xi}(t)\|^2$$
$$- \mathcal{Q}_5\|\tilde{q}(t)\|^2 + \mathcal{Q}_6, \tag{91}$$

where $\mathcal{Q}_4 \triangleq \lambda_{\min}(\mathcal{Q}_2)$ and $\mathcal{Q}_6 \triangleq 2\|\tilde{w}(t)\|\|(I_{N_{\mathrm{F}}} \otimes \Gamma^{-1})\|_{\mathrm{F}}\dot{w}^*$ with $\|\tilde{w}(t)\| \leq \tilde{w}^*$ and $\|\dot{w}(t)\| \leq \dot{w}^*$. Now, it shows that $\dot{\mathcal{V}}(e_{\mathrm{e}}(t), \tilde{\xi}(t), \tilde{w}(t), \tilde{q}(t)) < 0$ when $\|e_{\mathrm{e}}(t)\| \geq \psi_1$, $\|\tilde{\xi}(t)\| \geq \psi_2$, or $\|\tilde{q}(t)\| \geq \psi_3$, where $\psi_1 \triangleq \sqrt{\mathcal{Q}_6/\lambda_{\min}(\mathcal{Q}_3)}$, $\psi_2 \triangleq \sqrt{\mathcal{Q}_6/\lambda_{\min}(\mathcal{Q}_4)}$, and $\psi_3 \triangleq \sqrt{\mathcal{Q}_6/\lambda_{\min}(\mathcal{Q}_5)}$. This argument proves uniform ultimate boundedness of the closed-loop solution $(e_{\mathrm{e}}(t),$

$\tilde{\xi}(t), \tilde{w}(t), \tilde{q}(t))$ for all initial conditions (Khalil, 1996; Lavretsky & Wise, 2013).

■

The computation of the ultimate bound is presented through the next corollary.

Corollary 5.1: *Consider a multivehicle system consisting of N_F uncertain vehicles with the dynamics given by* (38)*, for $i = 1, \ldots, N_F$, with time-varying input disturbance, subject to Assumption* 4.1*, the ideal reference model given by* (49)*, the output emulator given by* (55)*, and the virtual vehicle-level controller given by* (46)*,* (47)*,* (51)*, and* (52)*. In addition, let the virtual local cooperative control for vehicle $i = 1, \ldots, N_F$, be given by* (62)*,* (63)*, and* (64)*, such that* (71) *is Hurwitz. Then, the ultimate bound of the solution $(e_e(t), \tilde{\xi}(t), \tilde{w}(t), \tilde{q}(t))$ is given by*

$$||e_e(t)|| \leq \tilde{\Phi}\lambda_{\min}^{-\frac{1}{2}}(P), \quad t \geq T \tag{92}$$

$$||\tilde{\xi}_e(t)|| \leq \tilde{\Phi}\lambda_{\min}^{-\frac{1}{2}}(\mathcal{P}), \quad t \geq T \tag{93}$$

and

$$||\tilde{q}_(t)|| \leq \tilde{\Phi}\lambda_{\min}^{-\frac{1}{2}}(\tilde{P}), \quad t \geq T \tag{94}$$

and the ultimate bound of the system error between the uncertain dynamical system and the ideal reference model is expressed as

$$\|e(t)\| = \|q(t) - q_m(t)\| \leq \tilde{\Phi}\left[\lambda_{\min}(P) + \lambda_{\min}(\tilde{P})\right]^{\frac{1}{2}}, \tag{95}$$

where $\tilde{\Phi} \triangleq [\lambda_{\max}(P)\psi_1^2 + \lambda_{\max}(\mathcal{P})\psi_2^2 + \lambda_{\max}(\Gamma^{-1})\tilde{w}^{*2} + \lambda_{\max}(\tilde{P})\psi_3^2]^{\frac{1}{2}}$.

Proof: It follows from the proof of Theorem 5.1 that $\dot{\mathcal{V}}(e_e(t), \tilde{\xi}_e(t), \tilde{w}(t), \tilde{q}(t)) < 0$ outside the compact set given by $\mathcal{S} \triangleq \{(e_e(t), \tilde{\xi}_e(t), \tilde{q}(t)) : \|e_e(t)\| \leq \psi_1\} \bigcap \{(e_e(t), \tilde{\xi}_e(t), \tilde{q}(t)) : ||\tilde{\xi}_e(t)|| \leq \psi_2\} \bigcap \{(e_e(t), \tilde{\xi}_e(t), \tilde{q}(t)) : \|q_e(t)\| \leq \psi_3\}$. That is, since $\dot{\mathcal{V}}(e_e(t), \tilde{\xi}_e(t), \tilde{w}(t), \tilde{q}(t)) < 0$, $\mathcal{V}(e_e(t), \tilde{\xi}_e(t), \tilde{w}(t), \tilde{q}(t))$ cannot grow outside $\mathcal{S}$, and hence, evolution of $\mathcal{V}(e_e(t), \tilde{\xi}_e(t), \tilde{w}(t), \tilde{q}(t))$ is upper bounded by $\mathcal{V}(e_e(t), \tilde{\xi}_e(t), \tilde{w}(t), \tilde{q}(t)) \leq \max_{(e_e(t), \tilde{\xi}_e(t), \tilde{q}(t)) \in \mathcal{S}} \mathcal{V}(e_e(t), \tilde{\xi}_e(t), \tilde{w}(t), \tilde{q}(t)) = \lambda_{\max}(P)\psi_1^2 + \lambda_{\max}(\mathcal{P})\psi_2^2 + \lambda_{\max}(\Gamma^{-1})\tilde{w}^{*2} + \beta\lambda_{\max}(\tilde{P})\psi_3^2 = \tilde{\Phi}^2$. Now, it follows from $e_e^{\mathrm{T}}(t)(I_{N_F} \otimes P)e_e(t) \leq \mathcal{V}(e_e(t), \tilde{\xi}_e(t), \tilde{w}(t), \tilde{q}_e(t))$, $\tilde{\xi}_e(t)^{\mathrm{T}}\mathcal{P}\tilde{\xi}_e(t) \leq \mathcal{V}(e_e(t), \tilde{\xi}_e(t), \tilde{w}(t), \tilde{q}_e(t))$, and $\tilde{q}^{\mathrm{T}}(t)(I_{N_F} \otimes \tilde{P})\tilde{q}(t) \leq \mathcal{V}(e_e(t), \tilde{\xi}_e(t), \tilde{w}(t), \tilde{q}_e(t))$, that $\|e_e(t)\|^2 \leq \frac{\tilde{\Phi}^2}{\lambda_{\min}(P)}$, $||\tilde{\xi}_e(t)||^2 \leq \frac{\tilde{\Phi}^2}{\lambda_{\min}(\mathcal{P})}$, and $\|\tilde{q}(t)\|^2 \leq \frac{\tilde{\Phi}^2}{\lambda_{\min}(\tilde{P})}$. Finally, since $e(t) = q(t) - q_e(t) + q_e(t) - q_m(t)$, and hence, $\|e(t)\| \leq \|q(t) - q_e(t)\| + \|q(t)_e - q_m(t)\| = \|e_e(t)\| + \|\tilde{q}(t)\|$, the ultimate bound given by (95) follows.

■

Remark 5.1: The convergence analysis for the containment problem follows the same approach as outlined in Albattat et al. (2018). For a thorough mathematical treatment of the containment problem, including the specific conditions under which convergence is guaranteed, the reader is referred to Albattat et al. (2018).

6. Illustrative numerical examples

To illustrate the effectiveness of the proposed output emulator-based observer-free adaptive control $(OF)^2AC$ for multivehicle systems, we present the following two examples, where we consider a line graph structure consisting of leader and follower vehicles. In particular, for each follower vehicle, the dynamics are governed by (12) and (13), with

$$A = \begin{bmatrix} 0 & 1 \\ 1 & 1 \end{bmatrix}, \quad B = \begin{bmatrix} 0 \\ 1 \end{bmatrix}, \quad C = \begin{bmatrix} 1 & 0 \end{bmatrix}, \tag{96}$$

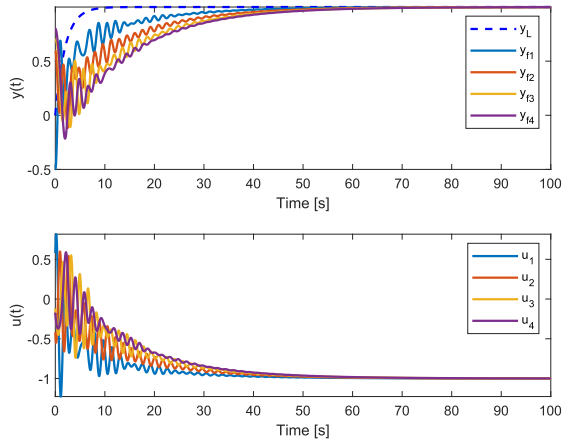
and varying vehicle-level uncertainties given by $w_1(t) = 0.4\sin(0.4t)$, $w_2(t) = 0.6\sin(0.2t)$, $w_3(t) = 0.4\sin(0.2t)$, $w_4(t) = -0.6\sin(0.4t)$. The initial conditions are $q_{10}^T = [0.5, 0]$, $q_{20}^T = [0.6, 0]$, $q_{30}^T = [0.7, 0]$, and $q_{40}^T = [0.8, 0]$. For the leader vehicle, the dynamics are governed by (31) and (32), with parameters $A_L = -0.5$, $B_L = 0.5$, $C_L = 1$, and initial condition $x_{L1}(0) = 0$. We set $\lambda = 10$ and define the system matrix:

$$A_m = \begin{bmatrix} 0 & 1 \\ -1 & -2 \end{bmatrix}, \tag{97}$$

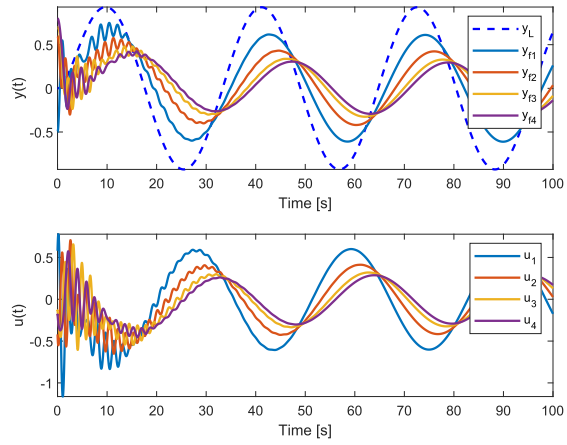
which results in the nominal feedback gains $K_q = [-1, -1.5]$ and $K_v = 0.5$. For the cooperative control design, we choose $K_c = 1.5$, $\zeta = 1.5$, $\eta = 2$, and $\delta = 5$. In the adaptive control design, we use $\gamma = 80$, $R = I_2$, and

$$P = \begin{bmatrix} 1.5 & 0.5 \\ 0.5 & 0.5 \end{bmatrix}. \tag{98}$$

The controller parameters are selected based on their distinct roles in stability and performance. The reference model A_m is chosen to specify the desired



(a) Step reference command (no disturbance)



(b) Sine-wave reference command (no disturbance)

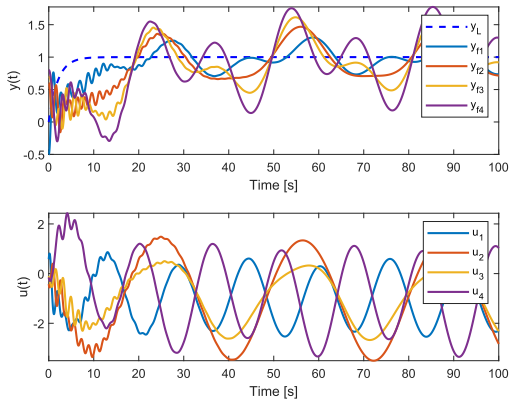
Figure 1. Responses of $y(t)$, $y_L(t)$, and $u(t)$ under nominal conditions (no input disturbance), showing accurate tracking of the reference command. (a) Step reference command (no disturbance). (b) Sine-wave reference command (no disturbance).

closed-loop dynamics, and the matrix P is obtained from the associated Lyapunov equation to guarantee stability. The adaptive gain γ regulates the adaptation rate, selected to balance fast uncertainty compensation and avoidance of oscillatory behaviour, while R is chosen as a positive definite weighting matrix. The cooperative gains K_c, ζ, η, and δ are selected to ensure convergence of the coordination error. In addition, the parameter selection follows standard Lyapunov-based design principles, ensuring stability while allowing performance tuning through a limited number of gains. Notably, the introduction of the output emulator improves transient smoothness without requiring retuning of these parameters, highlighting the structural advantage of the proposed approach. Finally, for each second-order follower vehicle with $d = 1$, the actual control signals from (77) take the form of an adaptive proportional-integral-derivative (PID) structure as given by

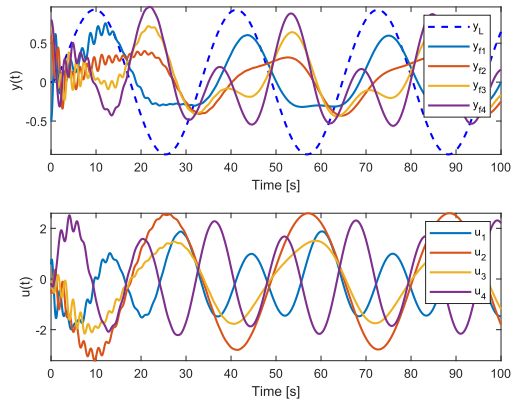
$$u_i(t) = \dot{\phi}_i(t) + 2\lambda\phi_i(t) + \lambda^2 \int_0^t \phi_i(\sigma_1)\, \mathrm{d}\sigma_1, \quad t \geq 0. \tag{99}$$

In this section, we demonstrate the effectiveness of the proposed output emulator-based $(\mathrm{OF})^2$AC method by considering both step and sine wave reference commands. For clarity of presentation, the simulations consider second-order linear follower dynamics; however, the proposed control framework is applicable to a broader class of higher-order and uncertain systems as developed in the theoretical sections. In addition, the number of agents is selected for clarity of visualisation; however, the proposed distributed control structure scales with network size, as each agent relies only on local neighbour information.

Example 6.1: In the first example, we assume a line graph consisting of four follower vehicles and one leader, with the objective of tracking a given reference command $c_1(t)$, $t \geq 0$. The closed-loop system response and the corresponding control signal are depicted in Figure 1. The proposed controller successfully drives the output of the multivehicle system to the desired reference command in the absence of input disturbances. When the $(\mathrm{OF})^2$ controller is applied without the adaptive component, Figure 2 illustrates an undesirable closed-loop response in the presence of disturbances affecting the follower vehicles. Subsequently, we introduce the $(\mathrm{OF})^2$AC controller, incorporating the adaptive mechanism, and the resulting closed-loop response and control signal are shown in Figure 3. Although the proposed controller improves disturbance rejection and command following, the response still exhibits noticeable high-frequency oscillations. To mitigate these oscillations, the output emulator-based adaptive control with $L = 1$ is introduced for both step and sine-wave reference commands. The controller parameters remain unchanged between Figures 3 and 4, and the only modification is the inclusion of the output emulator. The resulting behaviour shows a clear attenuation of high-frequency oscillations in the control signal while preserving tracking performance. In particular, the control input $u(t)$ exhibits smoother behaviour with

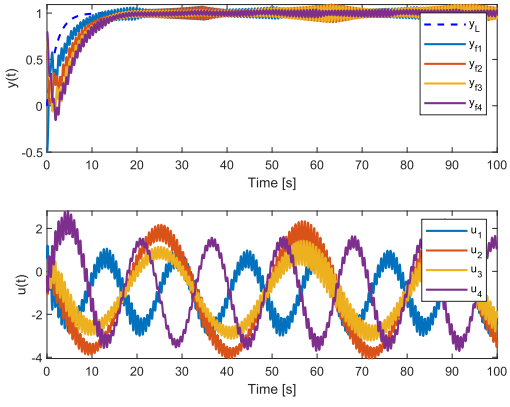


(a) Step reference command (in the presence of input disturbance, no adaptation)

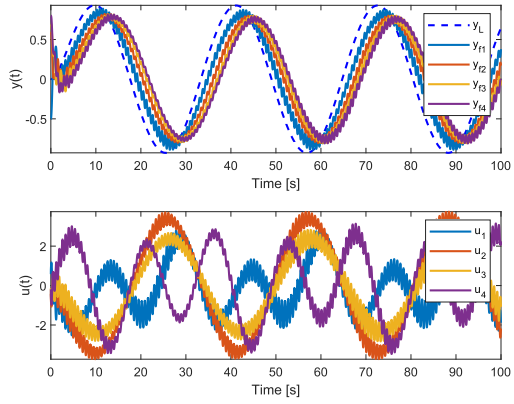


(b) Sine-wave reference command (in the presence of input disturbance, no adaptation)

Figure 2. Responses of $y(t)$, $y_L(t)$, and $u(t)$ in the presence of input disturbance without adaptation, illustrating degraded tracking performance and sensitivity to disturbances. (a) Step reference command (in the presence of input disturbance, no adaptation). (b) Sine-wave reference command (in the presence of input disturbance, no adaptation).



(a) Step reference command (in the presence of input disturbance, adaptive control without emulator)

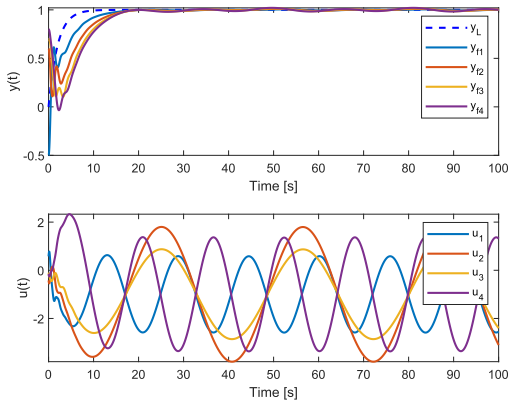


(b) Sine-wave reference command (in the presence of input disturbance, adaptive control without emulator)

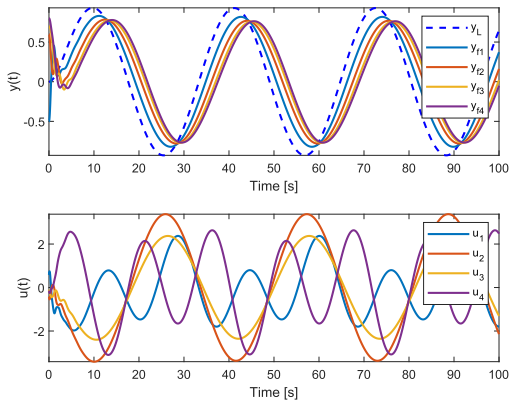
Figure 3. Responses of $y(t)$, $y_L(t)$, and $u(t)$ under $(OF)^2AC$ without emulator in the presence of input disturbance, showing improved disturbance rejection but noticeable high-frequency oscillations. (a) Step reference command (in the presence of input disturbance, adaptive control without emulator). (b) Sine-wave reference command (in the presence of input disturbance, adaptive control without emulator).

reduced oscillatory content, as evidenced by a decrease in its peak-to-peak amplitude compared to Figure 3. Unlike conventional adaptive controllers that rely on low-pass filtering or gain reduction to suppress oscillations, the proposed method achieves smooth control action through structural modification via the output emulator. Notably, unlike observer-based approaches, the proposed method does not require state estimation, thereby avoiding additional observer dynamics and potential estimation errors. Furthermore, Figures 2–4 illustrate a progressive transition from non-adaptive control to adaptive control and finally to the proposed emulator-based design. This confirms that the performance improvement is achieved through structural modification rather than parameter retuning.

Example 6.2: In the second example, we examine a system consisting of four follower vehicles and two leaders, each with distinct reference commands. In this configuration, the leaders define a convex hull toward which the followers are expected to approximately converge. The output emulator-based adaptive control strategy is applied using the same parameter settings as in Example 6.1. For the case of a constant reference command, we consider $c(t) = [1,\ 0.8]^{\mathrm{T}}$, as illustrated in Figure 5(a). In Figure 5(b), we investigate the case of time-varying reference commands, defined as $c_i(t) =$

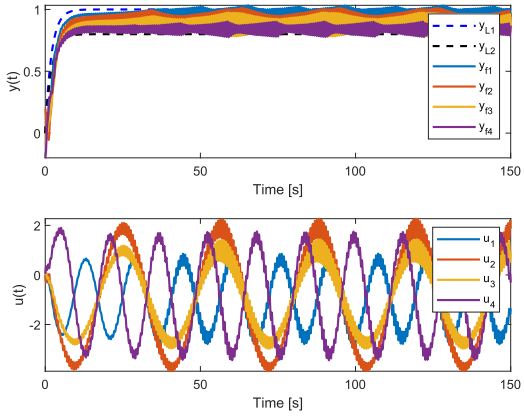


(a) Step reference command (in the presence of input disturbance, emulator-based adaptive control)

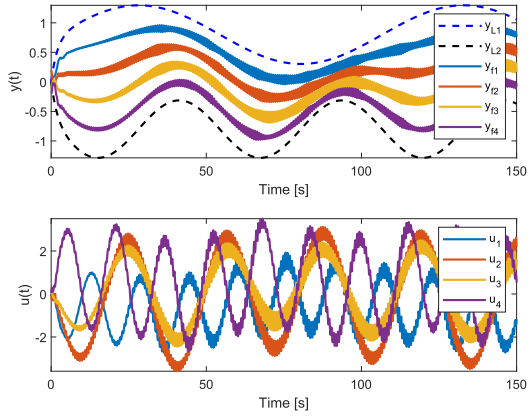


(b) Sine-wave reference command (in the presence of input disturbance, emulator-based adaptive control)

Figure 4. Responses of $y(t)$, $y_L(t)$, and $u(t)$ under the proposed emulator-based $(OF)^2AC$ in the presence of input disturbance, demonstrating improved tracking with significantly reduced oscillatory behaviour in the control input due to the inclusion of the output emulator. (a) Step reference command (in the presence of input disturbance, emulator-based adaptive control). (b) Sine-wave reference command (in the presence of input disturbance, emulator-based adaptive control).

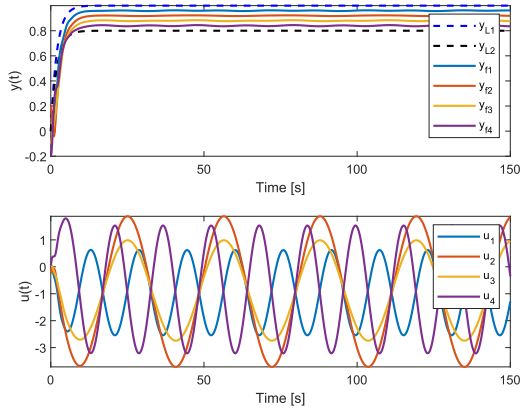


(a) Step reference commands for two leaders (no emulator)

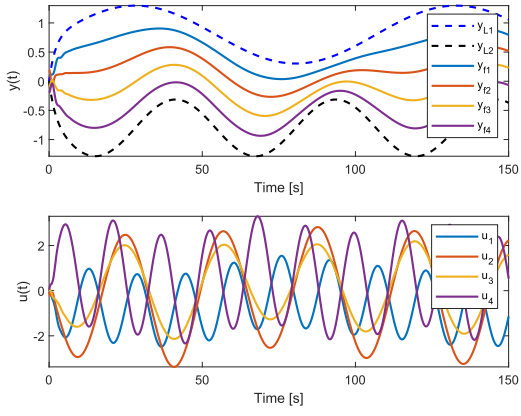


(b) Sine-wave reference commands for two leaders (no emulator)

Figure 5. Responses of $y(t)$, $y_L(t)$, and $u(t)$ for the two-leader containment scenario without emulator, showing containment within the convex hull with noticeable oscillations. (a) Step reference commands for two leaders (no emulator). (b) Sine-wave reference commands for two leaders (no emulator).



(a) Step reference commands for two leaders (with emulator)



(b) Sine-wave reference commands for two leaders (with emulator)

Figure 6. Responses of $y(t)$, $y_L(t)$, and $u(t)$ for the two-leader containment scenario under the proposed emulator-based adaptive control, demonstrating containment with smoother convergence and reduced oscillatory content. (a) Step reference commands for two leaders (with emulator). (b) Sine-wave reference commands for two leaders (with emulator).

$(-1)^{i+1}0.8 + (-1)^{i+1}0.5\sin((0.06 \cdot i)t)$, $i = 1, 2$. The results from both scenarios demonstrate that the follower vehicles converge to the convex hull generated by the leader outputs, thereby achieving the containment objective under both constant and time-varying reference commands. In the absence of the output emulator, as shown in Figure 5(a,b), the closed-loop response exhibits significant high-frequency oscillations in both the follower outputs and the control signals. For a fair comparison, all controller gains, initial conditions, and adaptive states are kept identical in both cases, and the only modification is the inclusion of the output emulator. With the inclusion of the output emulator-based reference system, as shown in Figure 6(a,b), the closed-loop response becomes significantly smoother, with reduced oscillatory content in the control input $u(t)$ while preserving containment performance. This improvement is attributed to the emulator-induced attenuation of high-frequency components in the reference dynamics, which reduces excitation of the adaptive loop and mitigates rapid fluctuations in the control signal. Consequently, the control input exhibits lower peak-to-peak amplitude compared to the non-emulator case.

7. Conclusion

In this work, we introduced a novel output emulator-based, observer-free output feedback adaptive control approach for continuous-time, minimum-phase, high-order linear multivehicle systems subject to exogenous disturbances. The proposed framework employs a nonminimal state-space representation for each follower vehicle and integrates local cooperative and vehicle-level controllers within a virtual control structure comprising nominal, adaptive, and cooperative components. The adaptive component compensates for disturbances in real time through an equivalent matched representation, while the cooperative component ensures convergence to the convex hull defined by the leaders. To improve transient performance, an output emulator reference system is incorporated to attenuate high-frequency oscillations through stable error feedback while preserving the observer-free architecture. Lyapunov-based analysis establishes uniform ultimate boundedness of the closed-loop system and boundedness of the parameter estimation error under a projection-based adaptive law. Although the framework relies on the standard assumption of bounded disturbance variation, it reduces tuning requirements while maintaining desirable transient performance. Finally, numerical examples demonstrate the effectiveness of the proposed method, and future work will focus on extensions to nonlinear vehicle dynamics and experimental validation.

Author contributions

CRediT: **Ali Albattat:** Conceptualization, Formal analysis, Investigation, Methodology, Software, Validation, Visualization, Writing – original draft, Writing – review & editing; **Tansel Yucelen:** Supervision, Writing – review & editing

Disclosure statement

No potential conflict of interest was reported by the author(s).

Data availability statement

The data that support the findings of this study are available from the corresponding author upon reasonable request. All simulations are reproducible using the models and parameters provided in the manuscript.

References

Albattat, A., Gruenwald, B., & Yucelen, T. (2017). Design and analysis of adaptive control systems over wireless networks. *Journal of Dynamic Systems, Measurement, and Control*, *139*(7), 074501. https://doi.org/10.1115/1.4035094

Albattat, A., & Yucelen, T. (2025). Output emulator-based observer-free distributed output feedback adaptive control for multivehicle systems. In *American Control Conference* (pp. 1858–1863).

Albattat, A., Yucelen, T., Gruenwald, B. C., & Jagannathan, S. (2017). An observer-free output feedback cooperative control architecture for multivehicle systems. In *ASME Dynamic Systems and Control Conference*, (Accepted).

Albattat, A., Yucelen, T., Gruenwald, B. C., & Sarangapani, J. (2018). Observer-free output feedback adaptive control for multivehicle systems with exogenous disturbances. In *AIAA Guidance, Navigation, and Control Conference*.

Antsaklis, P. J., & Michel, A. N. (2006). *Linear systems*. Birkhäuser.

Bernstein, D. S. (2009). *Matrix mathematics: Theory, facts, and formulas*. Princeton University Press.

Cai, H., Lewis, F. L., Hu, G., & Huang, J. (2017). The adaptive distributed observer approach to the cooperative output regulation of linear multi-agent systems. *Automatica*, *75*, 299–305. https://doi.org/10.1016/j.automatica.2016.09.038

Fax, J. A., & Murray, R. M. (2004). Information flow and cooperative control of vehicle formations. *IEEE Transactions on Automatic Control*, *49*(9), 1465–1476. https://doi.org/10.1109/TAC.2004.834433

Gibson, T. E., Annaswamy, A. M., & Lavretsky, E. (2012a). Adaptive systems with closed-loop reference models: Stability, robustness and transient performance. arXiv preprint arXiv:1201.4897.

Gibson, T. E., Annaswamy, A. M., & Lavretsky, E. (2012b). Improved transient response in adaptive control using projection algorithms and closed loop reference models. In *AIAA Guidance Navigation and Control Conference*.

Godsil, C., & Royle, G. (2001). *Algebraic graph theory*. Springer.

Haddad, W. M., & Chellaboina, V. (2008). *Nonlinear dynamical systems and control: A Lyapunov-based approach*. Princeton University Press.

Hu, J., & Zheng, W. X. (2014). Adaptive tracking control of leader–follower systems with unknown dynamics and partial measurements. *Automatica*, *50*(5), 1416–1423. https://doi.org/10.1016/j.automatica.2014.02.037

Khalil, H. K. (1996). *Nonlinear systems*. PrenticeHall.

Kim, Y., Mesbahi, M., & Hadaegh, F. Y. (2004). Multiple-spacecraft reconfiguration through collision avoidance, bouncing, and stalemate. *Journal of Optimization Theory and Applications*, *122*(2), 323–343. https://doi.org/10.1023/B:JOTA.0000042524.57088.8b

Lavretsky, E., Gadient, R., & Gregory, I. M. (2010). Predictor-based model reference adaptive control. *Journal of Guidance, Control, and Dynamics*, *33*(4), 1195–1201. https://doi.org/10.2514/1.46849

Lavretsky, E., & Wise, K. (2013). *Robust and adaptive control: With aerospace applications*. Springer.

Ma, C.-Q., & Zhang, J.-F. (2010). Necessary and sufficient conditions for consensusability of linear multi-agent systems. *IEEE Transactions on Automatic Control*, *55*(5), 1263–1268. https://doi.org/10.1109/TAC.2010.2042764

Mesbahi, M., & Egerstedt, M. (2010). *Graph theoretic methods in multiagent networks*. Princeton University Press.

Olfati-Saber, R., Fax, J. A., & Murray, R. M. (2007). Consensus and cooperation in networked multi-agent systems. *Proceedings of the IEEE*, *95*(1), 215–233. https://doi.org/10.1109/JPROC.2006.887293

Peng, Z., Wang, D., Zhang, H., & Sun, G. (2014). Distributed neural network control for adaptive synchronization of uncertain dynamical multiagent systems. *IEEE Transactions on Neural Networks and Learning Systems*, *25*(8), 1508–1519. https://doi.org/10.1109/TNNLS.2013.2293499

Pomet, J.-B., & Praly, L. (1992). Adaptive nonlinear regulation: Estimation from the lyapunov equation. *IEEE Transactions on Automatic Control*, *37*(6), 729–740. https://doi.org/10.1109/9.256328

Ren, W., Beard, R. W., & Atkins, E. M. (2005). A survey of consensus problems in multi-agent coordination. In *Proceedings of the American Control Conference* (pp. 1859–1864).

Sun, J., & Geng, Z. (2016). Adaptive consensus tracking for linear multi-agent systems with heterogeneous unknown nonlinear dynamics. *International Journal of Robust and Nonlinear Control*, *26*(1), 154–173. https://doi.org/10.1002/rnc.v26.1

Sun, J., Geng, Z., & Lv, Y. (2016). Adaptive output feedback consensus tracking for heterogeneous multi-agent systems with unknown dynamics under directed graphs. *Systems & Control Letters*, *87*, 16–22. https://doi.org/10.1016/j.sysconle.2015.10.007

Wang, J., Chen, K., & Ma, Q. (2014). Adaptive leader-following consensus of multi-agent systems with unknown nonlinear dynamics. *Entropy*, *16*(9), 5020–5031. https://doi.org/10.3390/e16095020

Yucelen, T., & Haddad, W. M. (2012). Output feedback adaptive stabilization and command following for minimum phase dynamical systems with unmatched uncertainties and disturbances. *International Journal of Control*, *85*(6), 706–721. https://doi.org/10.1080/00207179.2012.662721

Yucelen, T., & Haddad, W. M. (2013). Low-frequency learning and fast adaptation in model reference adaptive control. *IEEE Transactions on Automatic Control*, *58*(4), 1080–1085. https://doi.org/10.1109/TAC.2012.2218667

Yucelen, T., & Johnson, E. N. (2013). Control of multivehicle systems in the presence of uncertain dynamics. *International Journal of Control*, *86*(9), 1540–1553. https://doi.org/10.1080/00207179.2013.790077

Yucelen, T., & Pourboghrat, F. (2009). Active noise blocking: Non-minimal modeling, robust control, and implementation. In *American Control Conference* (pp. 5492–5497).